4. Accumulation rates of major constituents of hemipelagic sediments in the deep Alboran Sea: a centennial perspective of sedimentary dynamics

Masqué, P.[1,*,†], Fabres, J.[2,†], Calafat, A.M.[2], Canals, M.[2], Sanchez-Cabeza, J.A.[1], Sanchez-Vidal, A.[2], Cacho, I.[2,‡] and Bruach, J.M.[1]

[1] *Centre d'Estudis Ambientals, Departament de Física, Universitat Autònoma de Barcelona, E-08193 Bellaterra, Spain. Fax: 34-93-581-2155. E-mail: p.masque@uab.es*

[2] *GRC Geociències Marines, Dept. d'Estratigrafia, Paleontologia i Geociències Marines, Universitat de Barcelona, E-08028 Barcelona, Spain. Fax: 34-93-402-1340. E-mail: joan@geo.ub.es*

* *Corresponding author.*

[‡] *Present address: University of Cambridge, The Godwin Laboratory, Pembrooke Street, Cambridge, CB2 3SA, United Kingdom.*

[†] *These authors contributed equally to the work*

Acceptat per publicació a: **Marine Geology**, Setembre 2002

Abstract

The accumulation rates of sediment and major constituents in three different geographic areas of the Alboran Sea have been assessed by means of ^{210}Pb and ^{137}Cs concentration profiles. Mixing is present in the top layer of the sedimentary column, with mixing coefficients estimated to range from 0.2 to 15 $cm^2\ y^{-1}$. Overall, apparent sedimentation rates for the last 100 years range from 0.014 to 0.182 $g\ cm^{-2}\ y^{-1}$ and show a tendency to decrease with the distance to the coast and with the water column depth. However, specific characteristics of the sea floor for each physiographic environment govern the actual patterns of sediment accumulation. Particularly noticeable are the feeding role of submarine canyons, the trapping effect of slope terraces and the isolation caused by ridges. Sediment accumulation induced by turbiditic flows is also observed north of the Almeria-Oran area. Excess ^{210}Pb inventories and surface concentrations reveal a net effect of sediment focussing, and point to the role of bottom nepheloid layers in supplying a significant fraction of sediments to the deep areas. This is also evidenced by comparison of bottom sediment with sediment trap data available from the Malaga area. We estimate that the particle advective input below 30 meters above the bottom accounts for as much as 50-70% of the material that is ultimately deposited onto the sea floor. The greater abundance of lithogenic material in the Malaga zone (~80%) reflects its larger input in the western Alboran Sea. Conversely, carbonate contents increase from less than 20% in this area to about 30% in the Almeria-Oran zone, reflecting the lesser importance of the dilution by lithogenic components. Biogenic silica was only detected in some surface samples, and no significant preservation was observed below the Eh boundary. Abundance and accumulation rates of organic matter are in accordance with the spatial patterns of primary production in the Alboran Sea; higher in the western part, due to the presence of the Western Alboran Gyre. However, near bottom redistribution lead to the homogenisation of organic matter concentrations in bottom sediments of any given area. Finally, from comparisons with sediment trap data, the degradation of organic matter has been estimated to be approximately 30-40% of what reaches the bottom.

Keywords: Sediment accumulation rates, main constituents, ^{210}Pb, ^{137}Cs, organic carbon, Alboran Sea, Western Mediterranean.

4.1. Introduction

The Alboran Sea is the westernmost basin in the Mediterranean Sea (Figure 4.1). As a transitional area, between the Atlantic Ocean and the Mediterranean the Alboran Sea is characterised by highly dynamic and variable water mass movements that make it one of the most productive areas in the entire Mediterranean (Moran and Estrada, 2001). The preservation and export of organic matter and other suspended particles from the surface waters, where they are produced, down to the basin floor determines the role of the Alboran Basin as a potential carbon sink. Because of its hydrological situation and the features outlined above, the Alboran Sea was selected as one of the key areas to study sediment and major

constituents accumulation rates within the MTPII-MATER project (Mediterranean Targeted Project II - MAss Transfer and Ecosystem Response).

Natural and artificial radionuclides can be used as tracers of various marine processes. A pre-eminent example is the estimation of sediment mixing and accumulation rates at the sea floor using particle-reactive radionuclides (i.e. Guinasso and Shink, 1975; Benninger et al., 1979; DeMaster and Cochran, 1982; Cochran, 1985). ^{210}Pb, a member of the ^{238}U decay series, is especially useful to assess sedimentary processes on time scales of about 100 years, due to its half-life (22.3 y). ^{210}Pb is continuously introduced into the marine environment via the atmosphere, after decay from ^{222}Rn exhaled from the continental crust, and in the water column from in situ decay of dissolved ^{226}Ra. Due to ^{210}Pb having a higher affinity for fine-grained particles than ^{226}Ra, ^{210}Pb efficiently adsorbs to suspended and settling matter and sinks to the sea floor, where it is found in excess with respect to ^{226}Ra. This allows us to use excess ^{210}Pb to estimate recent (ca. 100 y) sedimentation and mixing rates through the implementation of appropriate mathematical models. This approach has previously been applied in the Western Mediterranean Sea by Zuo et al. (1997), Palanques et al. (1998), Radakovitch and Heussner (1999) and Sanchez-Cabeza et al. (1999a) amongst others. It has been often stated that independent evidence is needed to confirm the validity of the results obtained from ^{210}Pb methodologies (i.e. Smith, 2001). Some artificial radionuclides, such as ^{137}Cs, were introduced into the marine environment, in the fifties and sixties, as a consequence of the detonation of nuclear weapons in the atmosphere (Pappucci et al., 1996; UNSCEAR, 2000). The Chernobyl accident also contributed significantly to the total ^{137}Cs inventory in the Western Mediterranean Sea (Molero et al., 1999). Therefore, ^{137}Cs activity profiles in the sediment cores can provide us with up to three independent chronostratigraphic events: the beginning of atmospheric nuclear tests in 1954, the peak of nuclear detonations in 1963, and the Chernobyl accident in 1986.

The flux of major constituents (lithogenic particles, calcium carbonate, organic matter and opal) onto the sea floor can be calculated on the basis of the estimated sediment accumulation rates. In this study, relative and absolute compositions of sediment fluxes are used to infer the contributions of allochthonous sources and autochthonous production, and the transport/settling paths of sedimentary particles. Furthermore, major constituent fluxes onto the sea floor, together with fluxes through the overlying water column derived from sediment trap studies, are used to draw mass balances which are required to state the potential of the Alboran Basin as a sink for organic carbon and other major constituents. Indeed, organic carbon budget calculations are essential in estimating the contribution of continental margins and seas to anthropogenic CO_2 sequestration (Liu et al., 2000). We have fully applied the former background considerations and strategy to the study of eleven sediment cores from the Alboran Sea.

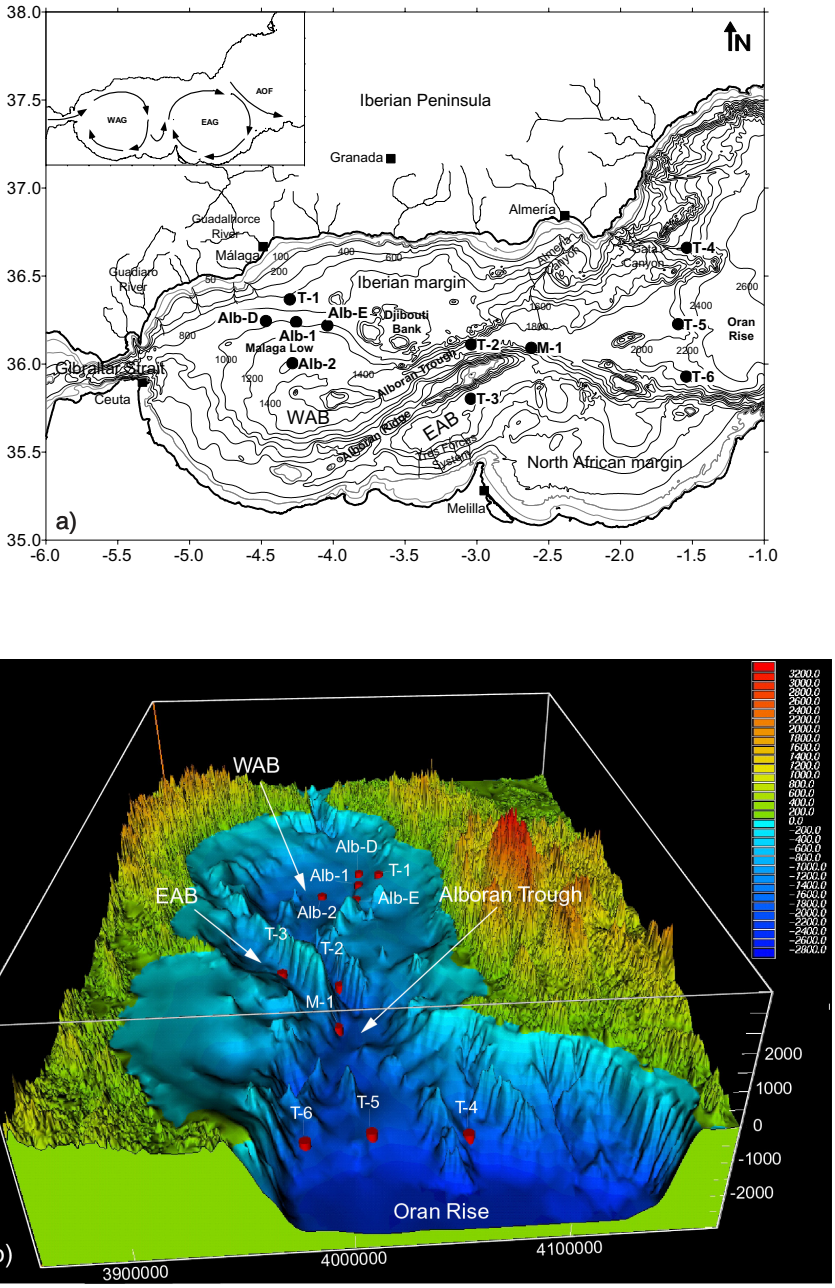

Figure 4.1. a) Map of the Alboran Sea indicating the location of the bottom sediment cores and the main physiographic features. Also shown are the main patterns of the surface circulation. WAG: Western Alboran Gyre, EAG: Eastern Alboran Gyre, AOF: Almeria-Oran Front, WAB: Western Alboran Basin, EAB: Eastern Alboran Basin. b) 3-D view from the E of the sea floor (blue tones) and coastal (green to red) relieves of the study area showing the location of the sediment cores.

4.1.1. Physiography and sediment types

The semi-enclosed Alboran Basin consists of a western and an eastern sub-basin. The Western Alboran Basin (WAB) is connected to the Atlantic Ocean through the Strait of Gibraltar to the west, and separated from the Eastern Alboran Basin (EAB) and the Algerian Basin by the volcanic heights of the Alboran Ridge and the Djibouti Bank, respectively (Figure 4.1). The WAB and the EAB are not to be

confused with the Western and Eastern Alboran Seas, which are simply the marine areas west and east of the Alboran Ridge, respectively. Between the heights of the Alboran Ridge and the Djibouti Bank there is the narrow Alboran Trough, which interconnects the WAB to the vast Algerian Basin. The Iberian and the North African margins bound the WAB to the north and the south, respectively. The Iberian margin is characterised by a narrow shelf (2-10 km width, 5 km average), a wide and smooth continental slope (20-50 km width and a 1:30 average gradient) and a wide base of the slope. The region between 4º and 4º 20'W is occupied by the small Malaga Low, which is separated from the nearby deeper basin floor by several low relief elevations. The basin floor is confined to the very central portion defined by the 1400 m isobath (Carter et al., 1972).

The EAB is a SW-NE elongated basin located between the Alboran Ridge and the North African Margin. It is bounded by the 1000 meter isobath and its maximum depth is slightly less than 1200 meters. The Tres Forcas system draining the African Margin feeds the EAB. North of the Alboran Ridge and east of the Djibouti Bank, the Alboran Trough broadens and opens towards the Oran Rise and the Algerian Basin. The easternmost Alboran Trough is surrounded by the steep slopes that fringe both the EAB and a broad region of ridges and valleys on the southern side, and a sinuous, canyon-incised slope on the northern side. The most prominent canyon on the northern margin is the Almeria Canyon. Further east, the Gata Canyon transports sediment to the Algeria bathyal plain.

Most of the Holocene sediments in the continental slope, the base of the slope and the basin floor in the Alboran Basin and the western termination of the Algerian Basin have been described as hemipelagic muds (Stanley et al., 1970; Huang and Stanley, 1972; Alonso and Maldonado, 1992; Ercilla et al., 1994). According to Rey and Medialdea (1989) the composition of these muds is controlled by river inputs, marine carbonate production in shallow areas, biogenic production in surface waters and the circulation of water masses. Graded turbiditic sands and silts are occasionally found interbedded with the hemipelagic muds, particularly in canyon influenced sectors, slope valleys and the upper slope (Stanley et al., 1970; Ercilla et al., 1994).

4.1.2. Circulation of water masses and primary production

The essential mechanism that determines the circulation patterns in the Alboran Sea is the water exchange that takes place through the Strait of Gibraltar. In addition, circulation in the Alboran Sea is strongly influenced by the rough seafloor topography, outlined in the previous section. The water masses identified in the Alboran Sea are: (i) the surface water of Atlantic origin, known as Modified Atlantic Water (MAW, $36.5 < S < 37.5$), which occupies the upper 200-300 m and flows from the Strait of Gibraltar to the Algerian Basin; (ii) the Surface Mediterranean Water (SMW) or Mediterranean Water (MW), which occupies the surface layer in areas not reached by the MAW; (iii) the Levantine Intermediate Water (LIW, $S>38.4$), characterised by relative temperature and salinity maxima, found between 200 and 600 m; and (iv) the Western Mediterranean Deep Water (WMDW), below the LIW, and characterised by decreasing temperature and salinity with depth (Gascard and Richez, 1985; Font, 1987; La Violette 1990; Viúdez et al., 1995).

The surface inflow of MAW usually describes two anticyclonic gyres of circa 100 km in diameter each, one in the Western Alboran Sea and the other in the Eastern Alboran Sea (Tintoré et al., 1988; Arnone et al., 1990) (Figure 4.1). While the Western Alboran Gyre (WAG) is an almost permanent fluctuating structure (La Violette, 1986, 1990; Parrilla and Kinder, 1987), the Eastern Alboran Gyre (EAG) is not a stable feature and, instead of the gyre, a jet along the African coast is sometimes observed (Viúdez and Tintoré, 1995). Complex three-dimensional adjustment processes take place at a variety of spatial and temporal scales and, given the very different densities of the water masses, strong density fronts might appear (Tintoré et al., 1994). An intense front often develops at the northern edge of the WAG, where MAW meets upwelled MW. MW upwelling is related to the offshore pushing of MAW by westerlies and/or to the fluctuations in the position of the WAG (Sarhan et al., 2000). This frontal structure is known as the Malaga Front. A second front is often located southeast of the Cape of Gata. When the EAG is formed, the flow of MAW coming from the Alboran Sea is driven off the Spanish coast (~ 2º W) towards the Algerian coast (~ 1º W). Since this jet of MAW meets the local MW flowing southwest along eastern Iberia, an intense density front appears in the upper 300 m, which is known as the Almeria-Oran Front (AOF) (Arnone and La Violette, 1986; Tintoré et al., 1988). In contrast to the general oligotrophic character of the Mediterranean, high productivity levels have often been recorded associated with the Malaga Front (Garcia-Gorriz and Carr, 1999; Baldacci et al., 2001; Ruiz et al., 2001) and the AOF (Lorenz et al., 1998). Furthermore, in the case of the Malaga Front, productivity in surface waters seems also triggered by nutrient inputs associated with fresh water discharge by local rivers (Fabres et al., 2002).

The surface water inflow in the Alboran Sea is balanced by a deep-water outflow of a time-variable mixture of LIW and WMDW across the Strait of Gibraltar (Kinder and Parrilla, 1987). Deep circulation in the Alboran Sea, and especially in the Western Alboran Basin, is affected by this outflow. A steady westward flow of LIW and WMDW has been recorded in several experiments, both along the Iberian and the North African margins (Gascard and Richez, 1985; Pistek et al., 1985; Parrilla et al., 1986; Fabres et al., 2002).

4.2. Materials and methods

4.2.1. Sampling

Eleven sediment cores (from 21 to 42 cm in length) were obtained using an eight tube maxicorer system from three geographical zones (Malaga, Alboran Island and Almeria-Oran) of the Alboran Sea during three cruises in October 1996, November 1997 and April 1998 (Figure 4.1 and Table 4.1). Cores T-1, ALB-1, ALB-D and ALB-E were collected in the WAB continental slope south of Malaga. Core ALB-2 was collected in the Malaga Low. Cores T-2 and T-3 were collected from the narrowest part of the Alboran Trough and from the floor of the EAB, north and south of the Alboran Island. Core M-1 was recovered from the easternmost, wider reach of the Alboran Trough, east of T-2 and south of the mouth of

Almeria Canyon. Cores T-4, T-5 and T-6 follow a meridian transect at 1.5ºW. In particular, core T-4 was retrieved at the axis of the lower Gata Canyon.

Once on board, sediment cores were visually described and redox potential (Eh) punch-in measurements were taken every centimetre from a replicate. The Eh equipment consisted of an Ingold Pt reference electrode and a Knick portable 651-mV meter. Eh data is given in raw mV units.

Immediately after retrieval, the replicate that had been visually described was subsampled in slices 0.5-2.0 cm thick using plastic tools, and stored in sealed plastic bags at 4 ºC for later analysis. The outer part of each section was removed to avoid contamination from contiguous sections during the coring operation. All analyses reported here, except for molecular biomarkers, were performed on samples from this single replicate. About half of each section was dried and homogenised to carry out radionuclide (^{210}Pb, ^{137}Cs and ^{226}Ra) and geochemical (total carbon, organic carbon, organic nitrogen and biogenic silica) analyses. The remaining wet non-homogenised sample was used for measurements of physical properties and determinations of grain-size. Since sampling procedures for molecular biomarkers exclude the use of plastic sampling instruments or bags, a different replicate core was sampled every 2-3 cm for molecular biomarker determination using metallic tools and glass containers.

Core	Location			Depth	Lenght	Sampling date
	Zone	Latitude N	Longitude W	(m)	(cm)	
T-1	Malaga	36º 22.05'	4º 18.14'	654	40	2-10-96
ALB-D	Malaga	36º 14.67’	4º 28.15’	946	42	27-4-98
ALB-1	Malaga	36º 14.31'	4º 15.52'	962	36	9-11-97
ALB-E	Malaga	36º 13.17’	4º 02.48'	1011	38	29-4-98
ALB-2	Malaga	36º 00.31'	4º 17.04'	1300	41	8-11-97
T-3	Alboran Island	35º 48.18'	3º 02.56'	1076	38	4-10-96
M-1	Alboran Island	36º 05.54'	2º 37.28'	1824	34	4-10-96
T-2	Alboran Island	36º 06.09'	3º 02.41'	1750	34	3-10-96
T-6	Almeria-Oran	35º 55.74'	1º 32.59'	1993	26	5-10-96
T-5	Almeria-Oran	36º 13.60'	1º 35.97'	2065	21	5-10-96
T-4	Almeria-Oran	36º 39.63'	1º 32.35'	2016	22	6-10-96

Table 4.1. Sampling locations of bottom sediment cores collected from the Alboran Sea.

4.2.2. Radiometric analyses

Determination of ^{210}Pb activities was accomplished through the measurement of its daughter nuclide ^{210}Po (Sanchez-Cabeza et al., 1998). Taking into account the time elapsed between sampling and analyses, ^{210}Pb was assumed to be in radioactive equilibrium with ^{210}Po in the sediment samples. Sample aliquots (200 mg) were totally digested by microwave heating in closed vessels at high pressure, after addition of ^{209}Po to each sample as an internal tracer. After digestion, samples were made 1 N with HCl and ^{209}Po and ^{210}Po were deposited onto silver disks at 60-70 ºC for 8 hours while stirring. Polonium

isotopes were counted with α-spectrometers equipped with low background silicon surface barrier (SSB) detectors (EG&G Ortec). Chemical recoveries ranged from 85 to 100% and energy resolutions ranged from 20 to 35 keV. For each batch of 10 samples, a reagent blank analysis was also carried out and used to correct sample activities. In all cases, blanks were comparable to detectors background (~2 10^{-5} s^{-1}).

The gamma-emitters ^{137}Cs and ^{226}Ra were measured by counting dried, homogenised samples in calibrated geometries for 2-3·10^5 seconds. A high purity intrinsic Ge detector, surrounded by a 12 cm lead shield, lined with 1 cm copper and 2 mm cadmium, and linked to an 8K Multi-Channel Analyser (MCA) was used. The resulting spectra were analysed using the Genie-PC Gamma Analysis Software (Canberra). ^{226}Ra was determined through the 351.9 keV and 609.4 keV gamma lines of ^{214}Pb and ^{214}Bi, respectively. Participation in several international intercomparison exercises organised by IAEA during the development of the work (i.e. IAEA-326, IAEA-327 and IAEA-368) and periodical analyses of certificate substances guarantee the quality of the results of the radiometric analyses.

Excess ^{210}Pb was calculated from the difference of total and supported ^{210}Pb, the latter in equilibrium with ^{226}Ra. Activities of ^{226}Ra were found to be constant along each core, and in accordance with supported ^{210}Pb activities from the deepest sediment samples, obtained using alpha measurements. In addition, a composite sample was prepared for each core, by combining a constant fraction of each section in which excess ^{210}Pb was present, and counted by gamma spectrometry. Individual ^{226}Ra activities were found to be well in agreement when comparing the results obtained using the different methodologies.

4.2.3. Calculation of sedimentation and mixing rates

Sediment reworking, owing to physical and/or biological agents, may affect the excess ^{210}Pb distribution along the sedimentary column. Therefore, any model of sedimentation must take into account this factor in order to avoid the overestimation of sediment accumulation rates (Benninger et al., 1979; Cochran, 1985). The main processes governing excess ^{210}Pb profiles in the seabed are sediment accumulation, radioactive decay and particle mixing (Goldberg and Koide, 1962). A one-dimensional advection-diffusion model is generally used to calculate the apparent sedimentation rate (S, in cm y^{-1}) and the mixing coefficient (D_B, in cm^2 y^{-1}) which describes the intensity of particle reworking:

$$\frac{\partial A}{\partial t} = D_B \frac{\partial^2 A}{\partial x^2} - S \frac{\partial A}{\partial x} - \lambda A \qquad (1)$$

where A (Bq kg^{-1}) is the excess ^{210}Pb concentration at depth x (cm), λ is the disintegration constant of ^{210}Pb (0.0311 y^{-1}), and S and D_B are assumed to be constant. This procedure has been applied to continental margin and deep-sea sediments (i.e. Guinasso and Shink, 1975; De Master and Cochran, 1982; Roberts et al., 1997; Masqué et al., 2002), including the Mediterranean Sea (Zuo et al., 1997; Sanchez-Cabeza et al., 1999a). The usual scheme is to consider the ^{210}Pb profile as a two layer system with a surface mixed layer (SML) extending to a distance L below the water-sediment interface and a

second layer below L where no mixing takes place. *S* can be determined from the non-mixed layer, where D_B is assumed to be negligible, or from the ^{137}Cs profiles, which may allow confirmation of results derived from ^{210}Pb. Where mixing is not present, equation (1) can be solved under the conditions of A = A_0 (x = L) and A $\rightarrow$ 0 (x $\rightarrow \infty$), by least-squares fitting of the equation

$$A = A_0 e^{-\frac{\lambda}{S} x} \qquad (2)$$

The sedimentation rate calculated in equation (2) can be introduced as a constant in equation (3) to determine D_B, also using least-square fitting:

$$A = A_0 e^{(S - \sqrt{S^2 + 4\lambda D_B})/2D_B) \cdot x} \qquad (3)$$

Since deep mixing cannot be ruled out, equation (2) provides us with an apparent sediment accumulation rate which may be considered as an upper limit (Benninger et al., 1979; Nittrouer et al., 1984). This procedure could also be used considering the accumulated mass (g·cm^{-2}) instead of the linear depth (cm) in order to take into account sediment porosity and compaction. The apparent sediment accumulation rate, so obtained, is expressed in terms of accumulated mass per unit area and per unit time.

4.2.4. Grain size, physical and geochemical analyses

Water content, porosity and wet and dry bulk densities were calculated from non-homogenised samples that were weighed before and after drying at 50 ºC until constant weight. An aliquot was also used for grain size determinations. A 10% H_2O_2 solution was added to 1-2 grams of sediment and ultrasounds were directly applied to the mixture in order to disaggregate the particles. After disaggregation was complete, samples were analysed using a Coulter LS100 with 100 channels resolution between 0.4 and 1000 µm. The results were recalculated to percentages of sand (> 63 µm), silt (63-4 µm) and clay (< 4 µm).

Each sample with excess ^{210}Pb was analysed with a Fisons 1500 elemental analyser for total carbon, organic carbon and nitrogen content using non treated and 25% HCl-treated samples (Nieuwenhuize et al., 1994). From the results, organic matter (organic carbon x 2), carbonate (total carbon - organic carbon x 8.33) and atomic C_{org}/N_{org} ratios values were calculated. Precision and accuracy of carbon and nitrogen content determinations were assessed through the analysis of the Canadian National Research Council certified estuarine sediment MESS-1 (Berman, 1990). Short term precision of carbon and nitrogen in a single run between consecutive runs (n = 8) averaged ± 2.3% and ± 5.0% of the measured values, respectively. Mid term precision (over the period between March and May 2000 (n=24)) was ± 2.9% for carbon and ± 8.4% for nitrogen. The accuracy of the method is excellent, as indicated by the correspondence between the measured carbon values, 3.05 ± 0.04%, and the certified carbon values, 2.99 ± 0.09%. Uncertainties in accuracy values represent confidence limits of 95%. Unfortunately, no certified N values were available for MESS-1.

For the analyses of particulate materials low in biogenic silica, such as those in this study, a new analytical method has been implemented by Fabres et al. (2002), based on the correction of Si contents by means of Al determination. This implies that the biogenic silica values have to be considered as minimum contents, as small amounts of aluminium could have been extracted from minerals other than aluminosilicates during the leaching process. The analytical procedure is as described in Fabres et al. (2002), excepting that a sediment aliquot of 20-30 mg, instead of 10-20 mg, was used for each analysis. Short term precision of opal measurements averaged ± 4.5% of the measured values when determined from the time consecutive replicate analysis (n= 3 or 4) of seven trap samples having a range of compositions from 1.1% to 14.7%. The opal detection limit associated to the detection limit of the ICP-AES system is 0.5% for a 20 mg sediment sample. Of the analysed samples only some from the topmost sections of the cores yielded values above the method detection limit.

Once all the major biogenic constituents (organic matter, carbonate and biogenic silica) were determined, the lithogenic content of each sample was determined by difference.

Concentrations of molecular biomarkers (C_{37} and *n*-nonacosane) were measured in all cores except ALB-1 with a 1- to -3 cm resolution over the depth region where excess ^{210}Pb was detected. The analytical procedure has been previously described (Villanueva and Grimalt, 1997; Cacho et al., 1999). Briefly, sedimentary lipids are extracted by sonification, the extracts are hydrolysed to eliminate wax ester interferences and, finally, derivatizated before instrumental analysis. The analyses were performed with a Varian Gas Chromatograph Model 3400 equipped with a septum programmable injector and a flame ionisation detector. Biomarker concentrations were determined by comparison of the peak area with an internal standard (*n*-hexatriacontane). Average reproducibility of molecular biomarkers concentrations was better than 10%.

4.3. Results

4.3.1. Sediment description

All the retrieved sediments were hemipelagic muds, that following the granulometrical classification of Shepard (1954) can be classified as silts except for some layers of sandy silts rich in sand-sized foraminiferal tests (cores ALB-1 and ALB-2) and sandy silts rich in coarse lithogenic particles (core T-4). Sandy silt levels are identified by relative maxima in sand contents (Figure 4.2). The recovered sediments were characterised by a dark to pale yellowish brown surface layer, 1 to 5 cm thick in all cores excepting for core T-4, where it was 12 cm thick. This surface layer overlaid olive grey to olive brown sediments. On the limit between the surface layer and the underlying sediments, a dark dusky yellowish brown band with black patches (0.5-1 cm thick) was also identified. All the redox potential profiles (Figure 4.2) exhibited gradually decreasing values closely related to colour evolution, excluding core T-4, where the redox profile showed a step-decreasing tendency. The Eh boundary (Eh=0) was located between the dark band base and 6 cm below. Therefore, the Eh boundary depth ranged from 1 to

8.5 cm, again with the exception of core T-4, where a depth of 15 cm was reached (Table 4.2). The dark band is explained as a layer where manganese dissolves in the reducing zone and diffuses upward above the Eh boundary, where it precipitates in the form of manganese oxides (Froelich et al., 1979).

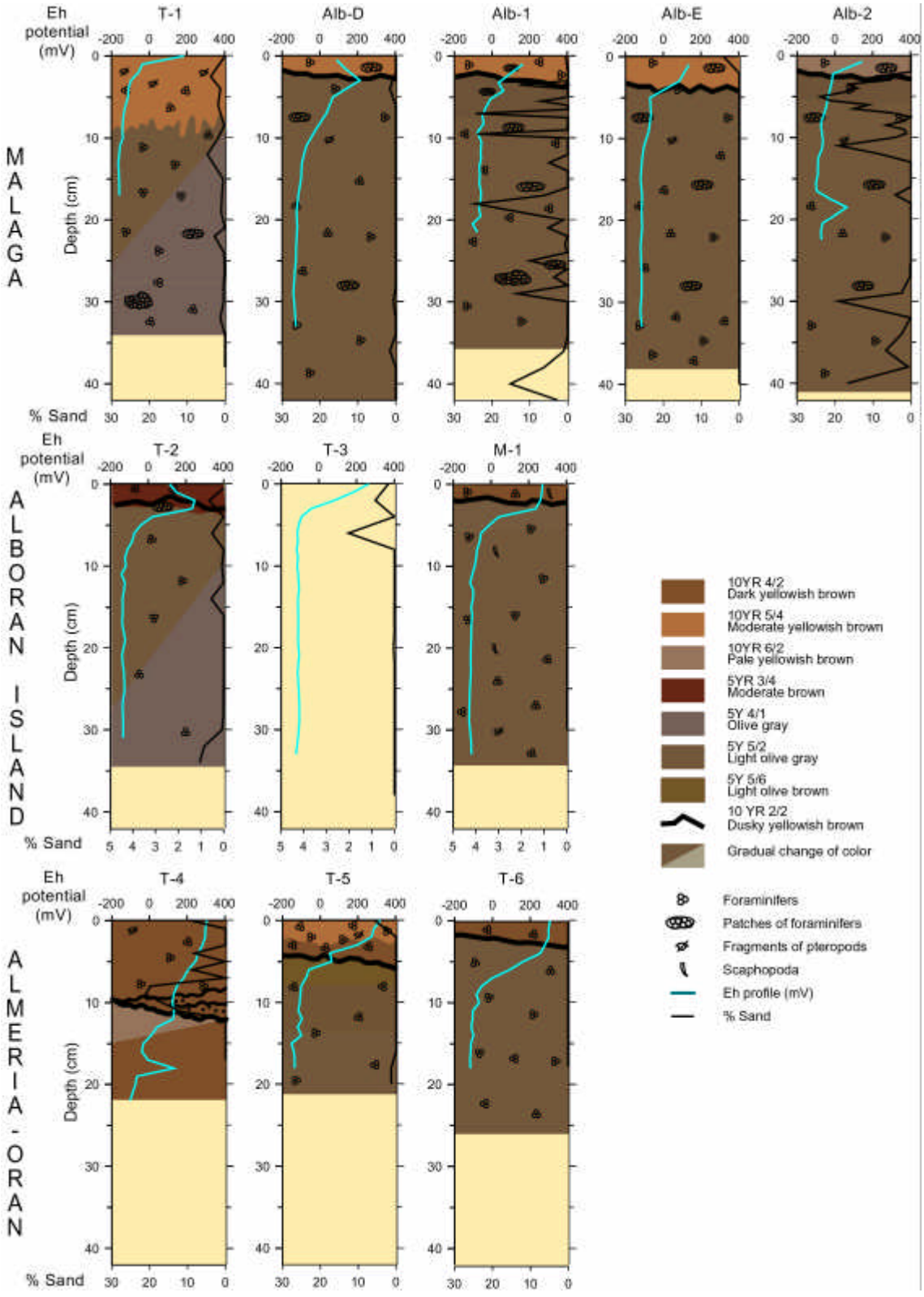

Figure 4.2. Visual descriptions and Eh and sand profiles in bottom sediment cores from the Alboran Sea.

4.3.2. ^{210}Pb and ^{137}Cs profiles

Mean supported ^{210}Pb concentrations obtained from alpha measurements ranged from 28 to 46 Bq kg^{-1} (Table 4.2). Excess ^{210}Pb and ^{137}Cs concentration profiles are shown in Figure 4.3. In the Malaga zone, excess ^{210}Pb horizons reached about 20 cm depth in all cores except that at station E, where it was observed down to only 15 cm depth. Surrounding the Alboran Island, excess ^{210}Pb was found until 24 cm depth in core T-3, and only down to 15 and 12 cm at stations T-2 and M-1, respectively. In the Almeria-Oran zone, excess ^{210}Pb reached only 6 cm at station T-4, and 12-13 cm at stations T-5 and T-6. Nine sediment cores were analysed for ^{137}Cs (Figure 4.3). The resolution of ^{137}Cs activity profiles was not high enough to clearly identify the 1963 and 1986 peaks caused by global fallout and the Chernobyl accident, respectively. However, the information obtained from ^{137}Cs profiles in terms of the depth to that is present allowed us to constrain and verify the mixing and sediment accumulation rates derived from the ^{210}Pb data (see below).

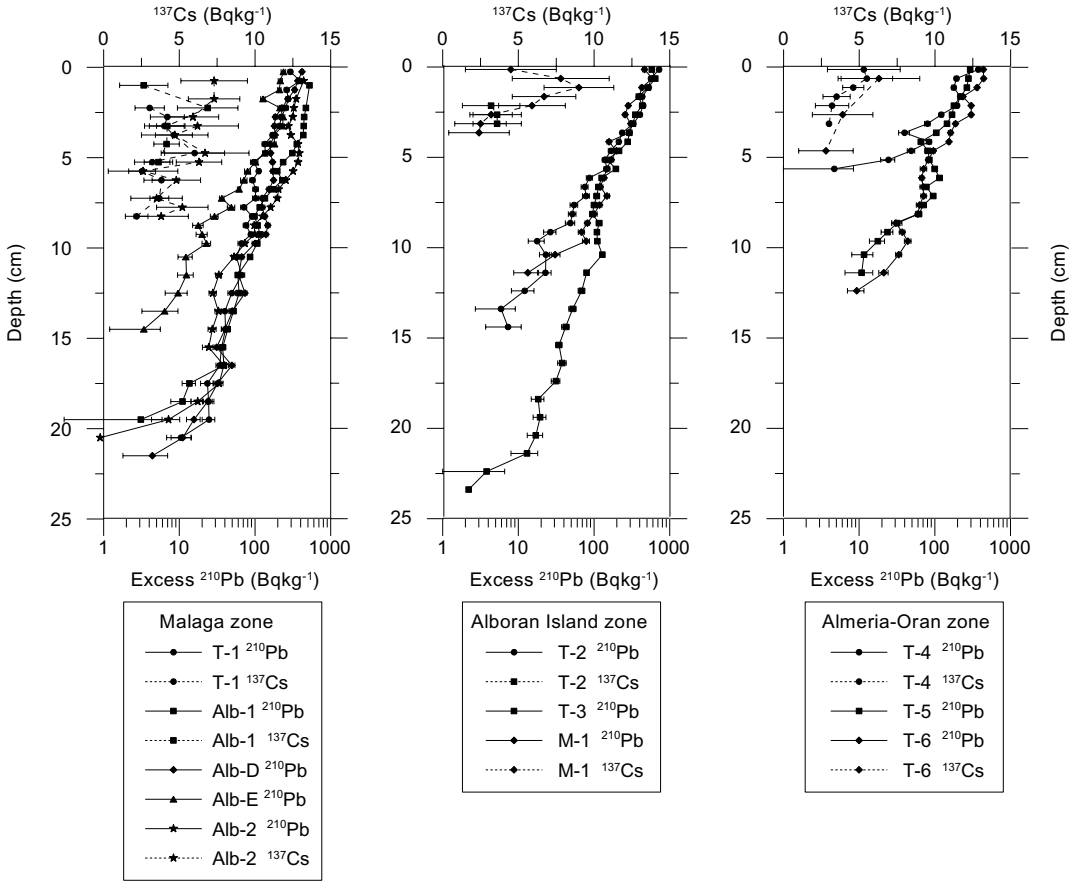

Figure 4.3. Excess ^{210}Pb and ^{137}Cs concentration profiles in bottom sediment cores from the Alboran Sea: (a) Malaga zone, (b) Alboran Island zone, and (c) Almeria-Oran zone. ^{137}Cs in cores T-3 and T-5 was only detected at a few depths, always within the first 5 cm.

Core	Supported ^{210}Pb	Excess ^{210}Pb				Mixing depth	Mixing coefficient	Mean SAR
		Horizon	Surface concentration	Inventory	Observed/Expected Inventories ratio			
	(Bq kg^{-1})	(g cm^{-2})	(Bq kg^{-1})	(kBq m^{-2})		(cm)	(cm^2 y^{-1})	(g cm^{-2} y^{-1})
T-1	34.6 ± 0.9	13.3	293 ± 19	10.66 ± 0.17	3.5	3.5	3.4	0.182 ± 0.011
ALB-D	34.8 ± 1.6	12.1	418 ± 17	11.35 ± 0.14	3.5	9.0	7.0	0.101 ± 0.010
ALB-1	34 ± 2	10.7	525 ± 25	13.40 ± 0.14	4.1	4.0	3.1	0.079 ± 0.005
ALB-E	31.7 ± 0.6	8.2	238 ± 16	5.97 ± 0.10	1.8	3.5	15.0	0.043 ± 0.002
ALB-2	32.0 ± 1.9	13.4	439 ± 10	14.57 ± 0.15	4.1	5.5	3.3	0.058 ± 0.002
T-3	34.4 ± 0.4	13.9	581 ± 41	15.1 ± 0.2	4.5			0.075 ± 0.007
M-1	46.4 ± 1.7	6.8	465 ± 29	11.03 ± 0.17	2.8			0.084 ± 0.006
T-2	33.1 ± 0.6	9.0	723 ± 43	10.22 ± 0.18	2.7	3.0	0.6	0.053 ± 0.002
T-6	27.6 ± 0.6	9.8	439 ± 19	9.68 ± 0.13	2.4	3.0	0.2	0.063 ± 0.006
T-5	31 ± 2	9.6	293 ± 15	8.50 ± 0.15	2.1	1.5	2.9	0.052 ± 0.005
T-4	42.9 ± 1.9	5.1	375 ± 21	5.15 ± 0.12	1.3	2.5	4.5	0.052 ± 0.008

Table 4.2. Mean 210Pb parameters in bottom sediment cores from the Alboran Sea, estimated mixing coefficients and mean apparent sediment accumulation rates (SAR).

4.3.3. C, N, carbonate, opal and molecular biomarkers

Profiles of organic carbon and nitrogen concentrations were similar in all cores, and results are shown in Figure 4.4. Maximum values were registered in the topmost part of each core and decreased by several tenths % until about the redox boundary (Figure 4.2). Below the redox boundary, values fluctuated slightly around a constant value or decreased but with a lower slope. The exception to that general trend was core T-3, for which higher variation in organic carbon concentrations were observed below the redox boundary. Organic carbon and nitrogen ranges were similar at each zone and occasionally between different zones. Organic carbon and nitrogen values in the Malaga zone ranged from 0.74 to 1.16% and 0.11 to 0.18%, respectively. In the Alboran island zone they varied from 0.70 to 1.53% and 0.11 to 0.18%. Finally, in the Almeria-Oran zone the range limits were 0.47-1.17% and 0.08-0.14%. The difference between the absolute maximum and minimum of atomic C/N ratios within each core was less than 2.5 units (Figure 4.4), except for cores T-3 and T-4, where fluctuations of more than 5 units were found. C/N ratios ranged from 6.6 to 10.0 in the Malaga zone, from 6.9 to 12.2 in the Alboran Island zone and from 6.0 to 11.8 in the Almeria-Oran zone.

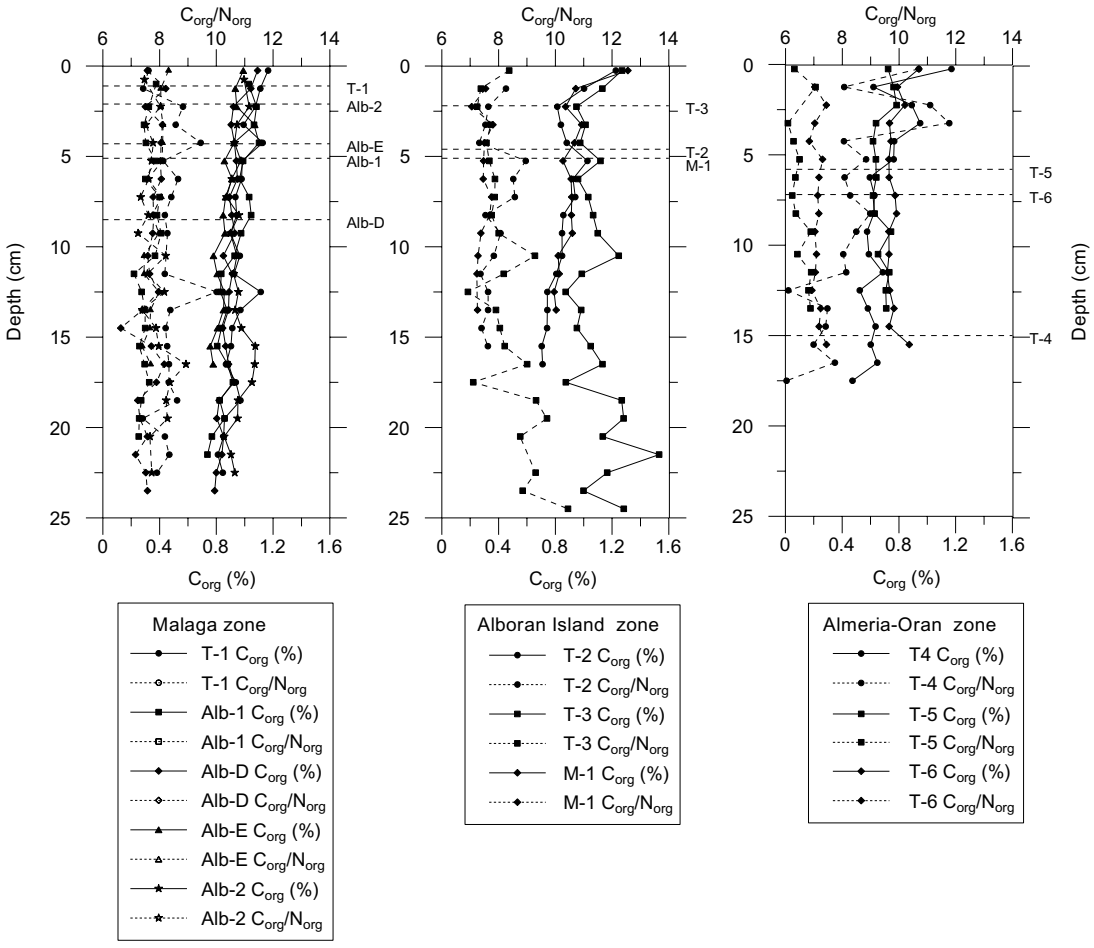

Figure 4.4. Organic carbon and C/N profiles in bottom sediment cores from the Alboran Sea: (a) Malaga zone, (b) Alboran Island zone, and (c) Almeria-Oran zone. Dotted lines indicate the oxic layer thickness.

Calcium carbonate, which constituted most of the total carbon, showed fairly constant concentrations throughout all the cores (Figure 4.5). The differences between the absolute maximum and minimum of each core were lower than 6%, except for cores T-4 and T-5, which showed differences of 13% and 9%, respectively. These larger differences are due to the presence of a broad minimum located around 8 cm in core T-4 and a sharper maximum located at the top of core T-5. Carbonate content ranged from 15% to 19% in the Malaga zone, from 19% to 27% in the Alboran Island zone and from 26% to 39% in the Almeria-Oran zone.

Opal analyses yielded values above the detection limit only for some samples above the redox boundary in sediments from the Malaga and the Alboran Island zones (Figure 4.5). The maxima opal contents in sediments from the Malaga zone were between 0.6% and 0.7%, while in sediments from the Alboran Island zone the maxima ranged from 0.7% to 1.0%.

C_{37} concentrations ranged from 57 to 789 μg g^{-1}, corresponding to cores T-4 and T-1, respectively. The three highest C_{37} values were observed in sediments recovered from the Malaga zone, while the three lowest corresponded to sediments from the Almeria-Oran zone. Concentrations of n-nonacosane ranged from 79 μg g^{-1} in core T-2, collected from the Alboran Island zone, to 278 μg g^{-1} in core ALB-E from the Malaga zone.

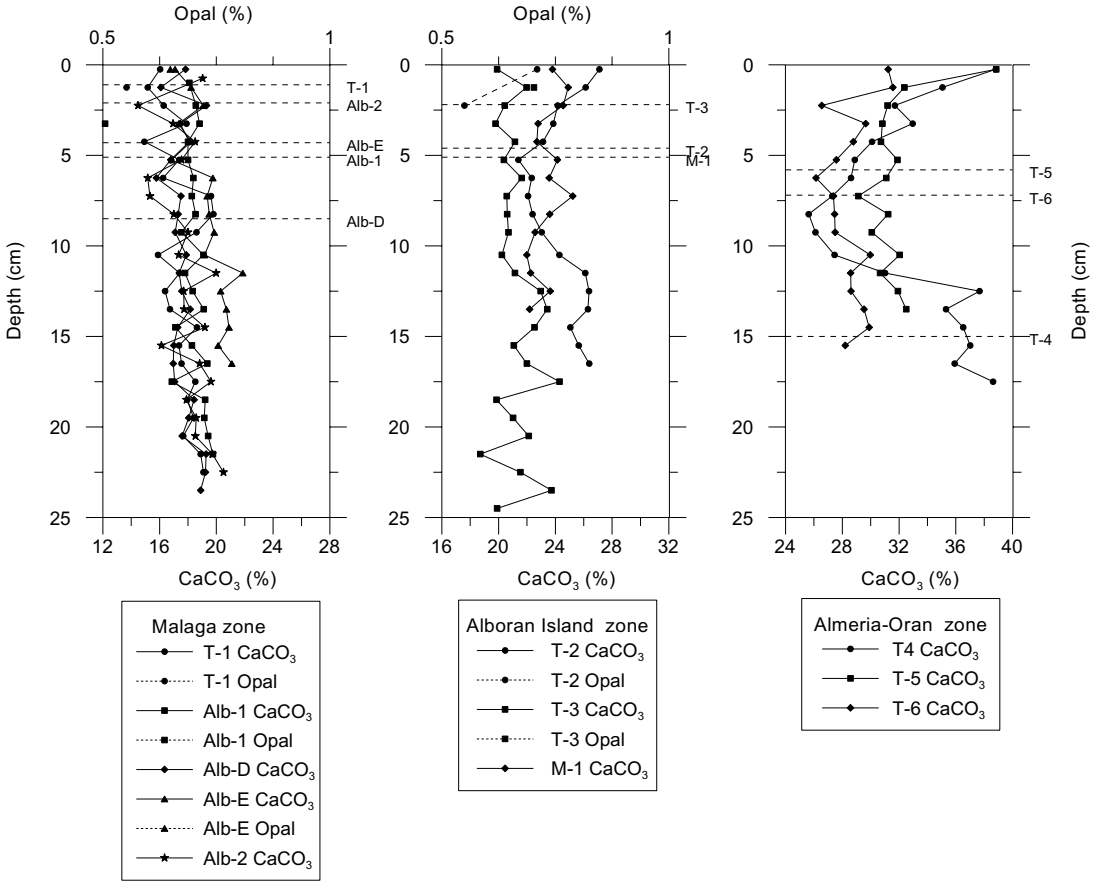

Figure 4.5. Calcium carbonate and opal profiles in bottom sediment cores from the Alboran Sea: (a) Malaga zone, (b) Alboran Island zone, and (c) Almeria-Oran zone. Dotted lines indicate the oxic layer thickness.

4.4. Discussion

4.4.1. Mixing and sediment accumulation rates

A surface mixed layer (SML) was identified in almost all ^{210}Pb profiles, occupying the topmost 1.5-5.5 cm. SML depths and mixing coefficients (calculated using equation 3) are shown in Table 4.2. The highest mixing rate was obtained for station ALB-E (15 $cm^2 \cdot y^{-1}$), being also remarkable at station ALB-D (7.0 $cm^2 \cdot y^{-1}$) and of about 3 $cm^2 \cdot y^{-1}$ or less for the rest of stations. Below the SML, an exponential decrease of excess ^{210}Pb concentration was observed in all cores, allowing us to consider these regions as not affected by deep mixing. It is worth noting that deviations from an exponential decrease were observed, mainly as local maxima of ^{210}Pb concentrations. We attribute these perturbations to infaunal organisms richer in ^{210}Pb that led to higher concentrations as bulk samples were used for analyses. Small deviations from a pure exponential decrease could be also attributed to short term changes in accumulation rates. However, since they were only punctual in character we maintain our assumptions to be still valid. Depths to which ^{137}Cs was detected (Figure 4.3), which would correspond to the early 50's, are consistent with apparent accumulation rates derived from ^{210}Pb, thus supporting the assumption of negligible deep mixing in the sediments.

Apparent mean sediment accumulation rates (SAR) (Table 4.2, Figure 4.6), ranged from 0.043 to 0.182 $g \cdot cm^{-2} \cdot y^{-1}$. When all cores are considered we observed a general trend by which SAR decreases as water column depth increases. This is specially clear in the Malaga zone, where SAR at station T-1, at 654 m, is more than double (0.182 $g \cdot cm^{-2} \cdot y^{-1}$) the SAR at the other stations, all of them deeper than 900 meters and located in the lower slope, the base of the slope and the basin floor. SAR differences between these stations are not so large but still noticeable, especially considering that they are located quite close together and at similar depths. The stations located deeper than 900 meters in the Malaga zone show a clear WNW-ESE decreasing pattern of SAR, being higher at stations ALB-D (0.101 $g \cdot cm^{-2} \cdot y^{-1}$) and ALB-1 (0.079 $g \cdot cm^{-2} \cdot y^{-1}$) than at stations ALB-2 (0.058 $g \cdot cm^{-2} \cdot y^{-1}$) and ALB-E (0.043 $g \cdot cm^{-2} \cdot y^{-1}$). In the Alboran Island zone, SAR are similar to those in the deeper part of the Malaga zone, higher at stations M-1 (0.084 $g \cdot cm^{-2} \cdot y^{-1}$) and T-3 (0.075 $g \cdot cm^{-2} \cdot y^{-1}$) than at station T-2 (0.053 $g \cdot cm^{-2} \cdot y^{-1}$). Finally, SAR in the Almeria-Oran zone are similar to the lowest SAR recorded in the two former zones, having the southernmost station a slightly higher value (0.063 $g \cdot cm^{-2} \cdot y^{-1}$) than the two other, which yield almost identical SAR (0.052 $g \cdot cm^{-2} \cdot y^{-1}$).

SAR distribution in hemipelagic sediments seems to be controlled by several factors, of which probably the most prominent is physiography. Zuo et al. (1997) showed a general trend in the Nortwestern Mediterranean by which sediment accumulation decreases with distance to the coast/continental margin. Our observations would appear to agree with the general principle that the SAR decreases with depth. The high SAR in station T-1 suggests that the upper slope area receives a higher amount of shelf-derived particles than the lower slope and basin. The upper slope is, in addition, more affected by near bottom transport of material than deeper areas. In situ transmisivity data following a

Core	Oxic layer thickness (cm)	Brown layer thickness (cm)	C (%)	Org N (%)	Org C (%)	C/N	C_{37} alkenones (ng g^{-1})	n-nonacosane (ng g^{-1})	Lithogenic (%)	$CaCO_3$ (%)	Organic matter (%)
T-1	1.1	1.0	3.06 ± 0.12	0.14 ± 0.01	0.97 ± 0.08	8.4 ± 0.6	457 ± 185	134 ± 27	80.6 ± 1.2	17.4 ± 1.3	1.93 ± 0.17
ALB-D	8.5	2.5	2.99 ± 0.07	0.13 ± 0.01	0.87 ± 0.04	7.5 ± 0.4	270 ± 32	155 ± 18	80.6 ± 0.6	17.7 ± 0.7	1.74 ± 0.08
ALB-1	5.1	3.0	3.11 ± 0.12	0.14 ± 0.01	0.91 ± 0.08	7.6 ± 0.3	n.m.	n.m.	79.8 ± 0.8	18.3 ± 0.8	1.81 ± 0.16
ALB-E	4.3	3.5	3.22 ± 0.15	0.13 ± 0.01	0.84 ± 0.04	7.8 ± 0.2	451 ± 65	175 ± 21	78.5 ± 1.3	19.8 ± 1.3	1.69 ± 0.07
ALB-2	2.1	2.0	3.07 ± 0.19	0.14 ± 0.01	0.96 ± 0.06	7.9 ± 0.4	240 ± 78	175 ± 22	80.5 ± 1.5	17.6 ± 1.5	1.92 ± 0.12
T-3	2.9	1.0	3.65 ± 0.13	0.15 ± 0.01	1.08 ± 0.16	8.4 ± 1.2	370 ± 72	113 ± 10	76.4 ± 1.2	21.4 ± 1.4	2.2 ± 0.3
M-1	5.1	2.0	3.68 ± 0.17	0.14 ± 0.01	0.88 ± 0.04	7.5 ± 0.2	302 ± 50	132 ± 25	74.9 ± 1.2	23.3 ± 1.2	1.76 ± 0.09
T-2	4.6	2.5	3.72 ± 0.15	0.12 ± 0.01	0.85 ± 0.09	8.0 ± 0.6	215 ± 66	134 ± 21	74.4 ± 1.8	23.9 ± 1.9	1.70 ± 0.19
T-6	7.2	3.0	4.14 ± 0.11	0.12 ± 0.01	0.74 ± 0.03	7.1 ± 0.1	163 ± 19	165 ± 37	70.3 ± 1.0	28.2 ± 1.0	1.49 ± 0.05
T-5	5.8	5.0	4.36 ± 0.13	0.12 ± 0.01	0.67 ± 0.05	6.5 ± 0.3	153 ± 20	158 ± 61	68.0 ± 1.0	30.7 ± 1.0	1.34 ± 0.12
T-4	15.0	2.0	4.1 ± 0.2	0.10 ± 0.01	0.69 ± 0.09	8.3 ± 0.4	65 ± 6	136 ± 36	69.9 ± 1.3	28.7 ± 1.2	1.38 ± 0.18

Table 4.3. Average C, N, molecular biomarkers and main constituent concentrations below the redox limit of the bottom sediment cores from the Alboran Sea (n.m.: not measured).

cross margin section from T-1 to ALB-1 and to ALB-2 showed higher relative particle concentrations in the bottom nepheloid layer at T-1 (Fabres et al., 2002). The slightly inclined slope terrace setting at T-1 may also favour enhanced sediment deposition. Also, it has been previously reported that sedimentation at depths of about 500-800 meters in continental slopes of the Western Mediterranean tends to be relatively high (Buscail et al., 1997; Sanchez-Cabeza et al., 1999a), a situation that has been attributed to the presence of a mid-slope depocenter.

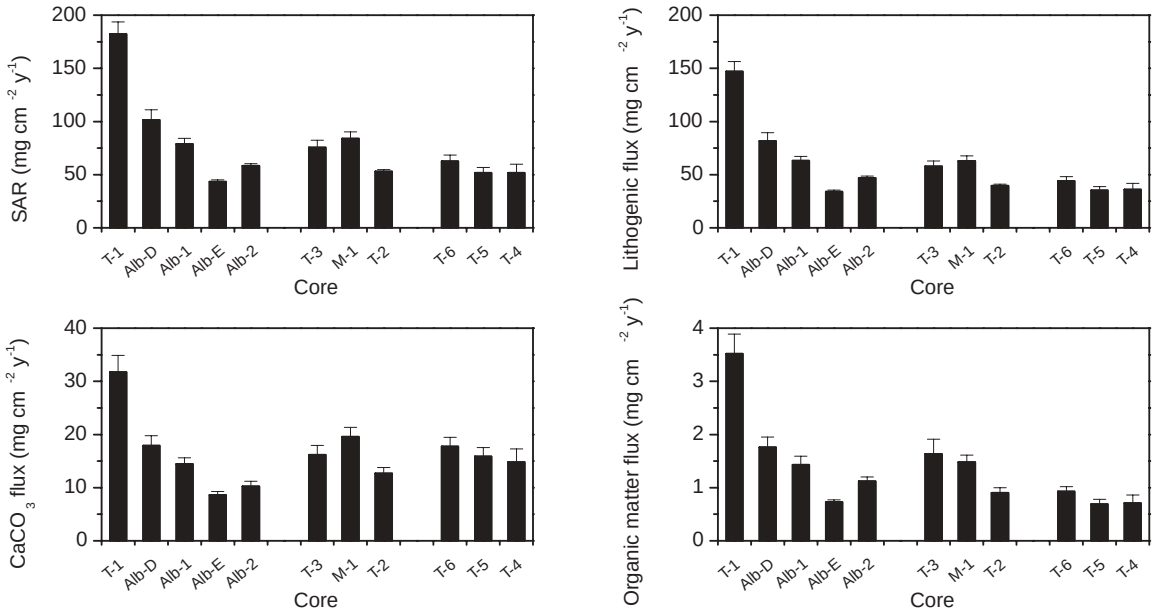

Figure 4.6. Mean sediment accumulation rates (SAR) and fluxes of the main constituents (lithogenic, calcium carbonate, organic matter) in bottom sediment cores from the Alboran Sea.

The differences in SAR between cores ALB-D, ALB-1 and ALB-E (Table 4.2, Figure 4.6), collected from similar depths, can be explained by the specific location of each core within the slope. The rather irregular slope presents the above-mentioned gentle slope terrace broadening eastwards (Figure 4.1). This terrace appears to act as a natural trap and retain the sediment derived from shallower areas. The wider the terrace the less sediment that would escape from it and be transferred downslope. The influence of this terrace is so noticeable that SAR in ALB-E is even lower than in ALB-2, which is located almost 300 meters deeper in the base-of-slope area. Furthermore, SAR distributions in the Malaga zone are probably affected by the presence of several submarine canyons incised in the upper slope, slightly west of the studied area (Ercilla et al., 1994). Submarine canyons are known to act as conduits of settling particles (Durrieu de Madron et al., 1990), and might preferentially feed the western midslope area where core ALB-D was retrieved. The thicker, youngest, seismic unit described by Ercilla et al. (1994) at the mouth of these canyons would appear to confirm a focussed sediment accumulation.

In the Alboran Island zone, SAR of core T-3, on the floor of the Eastern Alboran Basin, is similar to that of the ALB-1 core. It is noteworthy that both cores are located within the same depth range and at a similar distance from the shelf-break, confirming that these are important parameters in controlling SAR distribution in continental margins. The two other cores from the Alboran Island zone also deserve some discussion. Although M-1 is slightly deeper than T-2, SAR is about 60% higher, and

similar to that calculated for core T-3, which is 750 meters shallower. The high SAR in the M-1 area is interpreted as caused by the arrival of particles from the northern margins. In fact, core M-1 was retrieved south of where the Almeria Canyon meets the base of the slope. The Almeria Canyon system is the most significant morphological feature intersecting the continental margin off Almeria, and its sedimentary influence can be extended back to the entire Plio-Quaternary (Alonso and Maldonado, 1992). The low SAR in T-2 is explained due to its location between two slopes that are separated from shallower areas by seafloor ridges that hinder the direct arrival of suspended sediment from these areas.

The three cores in the Almeria-Oran zone have similar SAR, which are within the range obtained for T-2 and ALB-2. It would seem that SAR for all these cores are typical of relatively sediment starved base-of-slope and basin settings far from the direct influence of resuspension and downslope transfer from the shallow margins. Core T-4 is located in the axis of a major submarine canyon that delivers turbiditic flows to the base-of-slope (see next section). Nevertheless, this system is not directly fed by any significant fluvial system as is the case for the Almeria Canyon, and hemipelagic sedimentation processes may appear to be steady, as in any other area of the base-of-slope. The slightly higher accumulation rate in the southern core of the Almeria-Oran Zone, T-6, is probably due to its location besides a steep slope and to the resuspension and downslope transfer of the muddy sediments that accumulate on the embayments of the surrounding shelf areas (Leclaire, 1972). Resuspension and transfer of matter may be triggered by the sweeping effect of the strong eastward flowing Algerian current.

4.4.2. Excess ^{210}Pb inventories and scavenging from the water column

On steady state conditions, the atmospheric flux of ^{210}Pb to the ocean surface, F_{atm}, and the *in situ* production of ^{210}Pb from ^{226}Ra disintegration in the water column, F_{Ra}, would balance the decay of ^{210}Pb in the water column, D, and the export to bottom sediments, T_s:

$$F_{atm} + F_{Ra} = D + T_s \qquad (4)$$

F_{atm} is considered here to be 81.2 ± 1.4 Bq·m^{-2}·y^{-1}, as reported by Sanchez-Cabeza et al. (1999b) for the Northwestern Mediterranean. F_{Ra} and D have been estimated from data of ^{226}Ra and ^{210}Pb in the water column of the Alboran Sea that will be discussed in detail in Masqué et al. (in prep.).

Excess ^{210}Pb inventories in bottom sediment cores ranged from 5.15 ± 0.12 kBq·m^{-2} (core T-4) to 15.1 ± 0.2 kBq·m^{-2} (core T-3), corresponding to annual fluxes of excess ^{210}Pb to bottom sediments ranging from 158 to 462 Bq·m^{-2}·y^{-1}. Excess ^{210}Pb inventories in bottom sediments are higher than the expected export, T_s, calculated according to expression (4) (Table 4.2). In the Malaga zone, observed excess ^{210}Pb inventories are between 3 and 4 times higher than those expected from atmospheric input and ^{226}Ra and ^{210}Pb disintegration in the water column, with the exception of core ALB-E, for which the ratio is 1.8. The highest ratio (4.5) corresponds to core T-3, retrieved from the Alboran Island zone. The other two cores belonging to this zone, T-2 and M-1, also present inventories higher than expected. In the

Almeria-Oran zone, even though the inventories of excess ^{210}Pb are higher than those theoretically calculated, the ratios are not so large, especially for station T-4, where almost no extra excess ^{210}Pb has apparently been deposited. Overall, even if the effect of focussing of ^{210}Pb, and thus sediments, to all the studied areas is evident, differences on its magnitude are significant, being higher in the Malaga zone and lower in the Almeria-Oran zone. A general trend of decreasing influence of focussing with water column depth is also observed, although exceptions, probably related to the physiography, are identified. This is the case, notably, of station ALB-E.

Surface concentrations and total inventories of excess ^{210}Pb in the bottom sediments from the Malaga zone generally increase with water column depth, with the only exception of ALB-E, where both magnitudes are lower than expected for the general trend (Figure 4.7). Two processes influence the concentration of ^{210}Pb that is ultimately deposited onto the seabed. First, particles reaching the sea floor at deeper depths may be more enriched with ^{210}Pb due to longer residence times in the water column, where they scavenge dissolved ^{210}Pb. Second, the near-bottom advection of particulate matter, resuspended from the continental shelf and/or the upper slope and, a priori, poorer in ^{210}Pb, would lead to the dilution of ^{210}Pb concentration in bottom sediments; this effect would decrease in relation to distance from the coast.

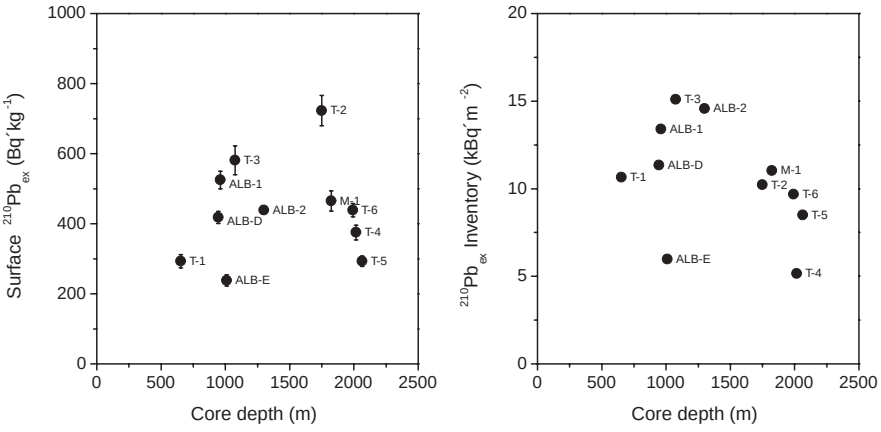

Figure 4.7. Surface concentration (a) and total inventory (b) of excess ^{210}Pb versus core depth in bottom sediment cores from the Alboran Sea

Excess ^{210}Pb concentrations in material collected by sediment traps in the Malaga zone (Masqué et al., in prep.) can be compared to the ^{210}Pb distributions in bottom sediment cores. Sediment traps were deployed for nearly a year (July 97 - May 98) at stations ALB-1 and ALB-2. The results as regards mass fluxes and major constituents are discussed in Fabres et al. (2002). At station ALB-1, mean concentrations of excess ^{210}Pb at 500 and 30 m above the bottom (mab) were 854 ± 9 and 1040 ± 9 Bq·kg^{-1}, respectively. At station ALB-2, mean concentrations were 744 ± 8, 936 ± 8 and 1084 ± 10 Bq·kg^{-1} at 800, 300 and 30 mab, respectively. Sediment traps deployed for two months (April and May 98) at 30 mab at stations ALB-D and ALB-E collected material with excess ^{210}Pb mean concentrations of 794 ± 13 and 812 ± 16 Bq·kg^{-1}, respectively. Thus, there is an apparent ^{210}Pb enrichment in sinking particles as they reach deeper waters.

It is also clear, on the other hand, that surface concentrations of ^{210}Pb in bottom sediment cores (Table 4.2) are significantly lower than those of particles collected by sediment traps deployed at only 30

mab. In general, given the sedimentation rates for these cores, the first half centimetre of sediments has been accumulated during a period of about 2 to 10 years, thus allowing for a certain decay of the ^{210}Pb activity in surface sediments. Also, mixing of the surface layer of bottom sediments would cause ^{210}Pb concentrations to be lower at the water-sediment interface. Settling material caught in traps may be finer than particles in surface bottom sediments, thus causing higher specific activities in traps. Furthermore, the above mentioned transmisivity data showed the presence of a bottom nepheloid layer (BNL) at stations T-1, ALB-1 and ALB-2 (Fabres et al., 2002). The particles transported by the BNL might therefore have a significant influence on the composition of the material that ultimately is deposited onto the sea floor, and could account for a fraction of the two to three-fold observed difference between sediment trap and surface bottom sediment ^{210}Pb concentrations. The lower than expected, if compared to station T-2, surface concentration of excess ^{210}Pb at station M-1 in the Alboran Island zone possibly reflects the influence of the near bottom supply of matter, that would also be responsible for its enhanced sedimentation rate. The excess ^{210}Pb inventory at station T-4 is significantly lower than those obtained for cores T-5 and T-6, retrieved at similar depths. This is probably related to the particular sedimentary conditions of the area as regards the occurrence of turbiditic flows that might supply old material, poor in excess ^{210}Pb (see next section).

4.4.3. Concentrations of major constituents and accumulation rates below the Eh boundary

Major constituents and organic carbon mean accumulation rates were calculated for every core by using the mean SAR and the average of the major constituent percentages in the section comprised between the Eh boundary and the deepest sample where excess ^{210}Pb was detected. In this section the abundance of major constituents does not vary significantly, since most of the early diagenetic activity occurs above the Eh boundary (Chester, 1990). Therefore, results represent a suitable approximation of what is exported from the water column to the sea floor and buried efficiently on a centennial time scale. The only exception to this flux calculation procedure was station T-4, of which a detailed discussion is given below.

To calculate and explain the major constituent accumulation rates, it is necessary to ascertain if the sediments have accumulated by true hemipelagic processes. Otherwise, inferences derived could yield erroneous conclusions about the mechanisms controlling particle fluxes. In the areas sampled, the thickness of the brown surface oxidising layer (Table 4.2), the gradually decreasing redox potential profiles (Figure 4.2), the accumulation rates (Table 4.2) and the organic carbon content (Figure 4.4) are typical for oxic/suboxic hemipelagic sediments (Chester, 1990). Huang and Stanley (1972), Alonso and Maldonado (1992) and Ercilla et al. (1994) have recognised the predominance of hemipelagic sedimentation processes during the last century to millennia in the slope, base-of-slope and basin areas of the Western and Eastern Alboran Sea.

Some properties of the section between 8 and 12 cm of core T-4 suggest that processes other than hemipelagic settling have contributed particles to the axis of the distal part of the Gata Canyon. The peculiar properties include dark coloured erosive discontinuities (Figure 4.2), absence of excess ^{210}Pb (Figure 4.3), higher sand and lower organic carbon and carbonate contents than the under and overlying sediments (Figures 4.2, 4.4 and 4.5); higher C/N values than the underlying section; and, finally, high constant values of redox potential. Both the physiographic setting and sediment characteristics suggest that this section may correspond to sediments accumulated from a turbiditic flow originating at the shelf break or on the upper slope, characterised by scattered volcanic rock outcrops (Zamarreño et al., 1993), where sediments richer in lithogenic, probably volcanic, constituents (poorer in carbonate and organic matter) and higher C/N ratios were originally deposited. Alonso and Maldonado (1992) also reported the contribution of turbiditic flows in delivering sediments to the base of the slope in the northern side of the Alboran Trough, south of the Gata Canyon, not far from where T-4 was retrieved. SAR for core T-4 was calculated from the section between 2 and 6 cm, which was considered to correspond to sediments accumulated by hemipelagic settling. Average values of main constituents were taken from the section between 4 and 8 cm on top of the turbiditic layer in order to estimate main constituent accumulation rates. This is not below the Eh boundary but is the deepest section not affected by the turbiditic event and for which an estimation of the sediment accumulation rate can be used.

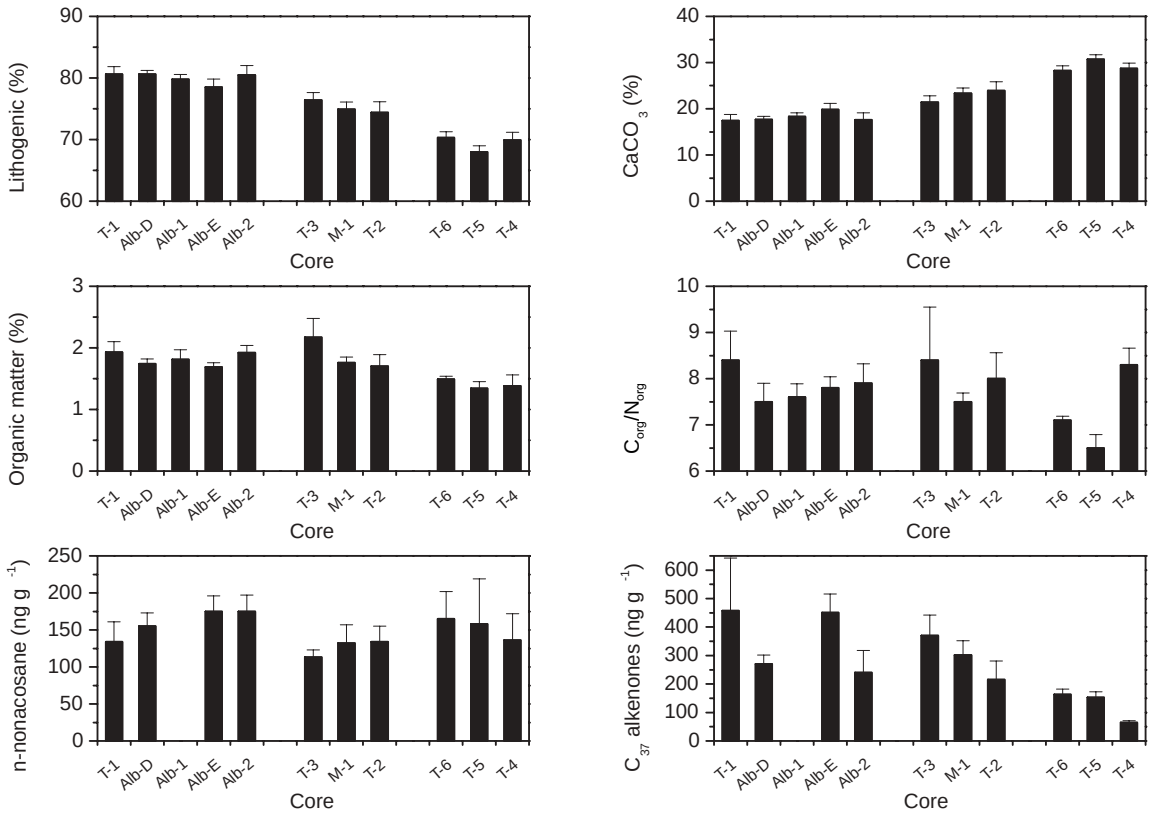

Figure 4.8. Mean concentrations of main constituents (lithogenic, calcium carbonate, organic matter), organic C/N ratio, C_{37} alkenones and n-nonacosane in bottom sediment cores from the Alboran Sea.

The average percentages of main constituents are given in Table 4.3 and plotted in Figure 4.8. The corresponding fluxes are shown in Figure 4.6, together with the SAR used to calculate them. The

distribution of main constituent fluxes is clearly influenced by the sediment accumulation rate and, therefore, by depth, distance from the margin and physiography. All the cores showed main constituent accumulation rates within the same range, except for core T-1, that recorded values twice or three times higher that the rest. However, variations in relative abundances of major constituents yielded significant differences that are not obvious if only SAR are considered.

The percentages of lithogenic constituents showed a clear decreasing pattern from west to east, with values close to 80% in the Malaga zone, 75% in the Alboran Island zone and 70% in the Almeria-Oran zone. These percentages, together with the estimated SAR, yield higher lithogenic accumulation rates, between 82 and 63 $mg \cdot cm^{-2} \cdot y^{-1}$, in cores ALB-D, ALB-1, M-1 and T-3, and lower values, between 47 and 34 $mg \cdot cm^{-2} \cdot y^{-1}$, in cores ALB-2, T-6, T-2, T-4, T-5 and ALB-E. The overall marked decrease in the lithogenic fraction towards the east, clearly reflects that the highest input of lithogenic particles in the Alboran Sea occurs at its western end (Stanley et al., 1975; Rey and Medialdea, 1989). Moreover, detailed comparisons between cores within the same zone allow us to identify the influence of local lithogenic sources and of physiographic control over the distribution of this lithogenic material. In the Malaga zone there is a smooth decrease in lithogenic content from west to east. This is attributed to the influence of the Guadiaro and Guadalhorce riverine inputs, northwest of the area from which the cores were retrieved, and the role of submarine canyons, located west of Malaga, as preferential conduits for the lithogenic material that reaches the outer shelf. In the Alboran Island zone, core T-3 has a slightly higher lithogenic content than the other two neighbouring cores, probably because of its closer location to the North-African coast and to the absence of any physiographic barrier that could hinder the arrival of particles, in contrast to core T-2. In the Almeria-Oran zone cores T-4 and T-6 show higher lithogenic contents than T-5, reflecting their closeness to the Iberian and North-African margins, respectively.

Carbonate percentages show an opposite trend to that of the lithogenic constituents, clearly increasing from west to east, with values slightly below 20% in the Malaga zone, between 21% and 24% in the Alboran Island zone and around 30% in the Almeria-Oran zone. Carbonate accumulation rates ranged from 9 to 20 $mg \cdot cm^{-2} \cdot y^{-1}$. Lowest values were recorded in cores ALB-E and ALB-2, with 8.6 and 10.3 $mg \cdot cm^{-2} \cdot y^{-1}$ respectively, while the other cores range from 12.7 to 19.6 $mg \cdot cm^{-2} \cdot y^{-1}$. This mirror trend with respect to lithogenic matter is interpreted as an effect of dilution. In general, the further from the lithogenic sources and margins, the higher the carbonate content is. The lack of preservation of any significant quantities of opal below the Eh boundary in the sediments, as compared to the fluxes measured in the water column (Fabres et al., 2002) (Table 4.4), allowed us to deduce that biogenic silica produced in the water column is not exported to the bottom sediments in any considerable quantity. Only above the Eh boundary of the cores from the Malaga and the Alboran Island zones is some opal accumulated, but no significant quantities seem to resist early diagenesis and remain preserved. Bárcena and Abrantes (1998) and Bárcena et al. (2001) have also reported low abundance of diatom valves in surface sediments of the Alboran Sea.

Organic matter percentages were lower in the Almeria-Oran zone, with values between 1.3 and 1.5%, compared to the other two zones, where they ranged from 1.7 to 2.2%. Organic matter accumulation rates and percentages were parallel to lithogenic accumulation rates. Cores ALB-D, ALB-1,

T-3 and M-1 showed values between 1.4 and 1.8 $mg \cdot cm^{-2} \cdot y^{-1}$ and cores ALB-2, T-6, T-2, T-5, T-4 and ALB-E showed values between 0.7 and 1.1 $mg \cdot cm^{-2} \cdot y^{-1}$.

4.4.4. Factors controlling organic matter accumulation rates

Organic matter concentrations in marine sediments are controlled by the interaction of different factors; the three major variables being input, preservation and dilution (Tysson, 2001). As regards the input of organic matter, autochthonous primary productivity is, on average, higher in areas where strong density fronts develop and where river discharges fertilise the surface waters. In the Alboran Sea this particularly applies to the northern edge of the WAG and, occasionally, to the Almeria-Oran Front. The annual primary production map for year 1991 derived from Coastal Zone Coastal Scanner (CZCS) images (Morel and André, 1991) and those for years 1998 and 1999 derived from SeaWiFS images (Falkowski et al., 2002) reveal higher annual production (200-450 g C m^{-2} a^{-1}) around the whole WAG and as far as the longitude of Melilla than in the Almeria-Oran Front (150-360 g C m^{-2} a^{-1}). Lower annual production in the AOF area is probably due to the higher temporal and spatial variability of this structure (not as stable as the WAG). C/N ratios are very similar in all the cores (6.5 - 8.4, Table 4.3) and in all cases below 10 indicating the dominant input of marine above terrestrial organic matter (Buscail et al., 1990). Nevertheless, most of them are higher than the Redfield ratio for marine phytoplankton (6.6), presumably indicating also some degradation of organic matter during its transfer through the water column. The overall distribution of organic matter percentages showed a clear decreasing trend from the Malaga and Alboran Island zones towards the Almeria-Oran Front, which seems to be the result of higher marine production in the Western Alboran Sea. This conclusion is further supported by the different distribution of *n*-nonacosane and of C_{37} concentrations, which are molecular biomarkers of terrestrial (Eglinton and Hamilton, 1967) and marine (Volkman et al., 1980) origin, respectively (Figure 4.8). The marine biomarker tracks the distribution of marine organic production with values in the Malaga and Alboran Island zones, doubling in average those from the Almeria-Oran zone. The terrestrial biomarker shows low homogeneous background values in all the cores, highlighting the low and non focused input or organic matter of terrestrial origin.

The redistribution of organic matter near the bottom by resuspension processes is probably partly responsible for the homogeneity of abundances of organic carbon within each physiographic zone. For example in the Malaga Zone, where disregarding the fact that the most productive areas are located on the periphery of the WAG and, therefore, over the shelf and upper slope, the core from the basin bottom (Alb-2) has a organic matter abundance similar to those retrieved from the slope.

The second factor that plays a key role in organic matter distribution in bottom sediments is preservation. Once organic matter reaches the bottom, it is subject to a certain degree of degradation. Degradation directly depends on the amount of oxygen available to oxidise the organic matter, which in turn depends on the SAR, that controls how long organic particles are exposed to an oxic environment (Figure 4.9a), and on the amount of dissolved oxygen in bottom waters. A comparison between the percentage and accumulation rate of organic carbon preserved in the sediment (below the Eh boundary)

and the thickness of the oxic layer (Figure 4.9b) reveals that, in general, the thicker the oxic layer the less organic carbon is preserved. There is also a relation between the percentage and accumulation rate of preserved organic carbon and the depth at which the core was retrieved (Figure 4.9c). The deeper the core the less organic carbon is preserved. This relation is linked, as mentioned above, to the higher production in WAB where the shallower cores were collected. Nevertheless, some influence of organic matter degradation during its transfer through water column or from shallower to deeper bottom areas cannot be ruled out.

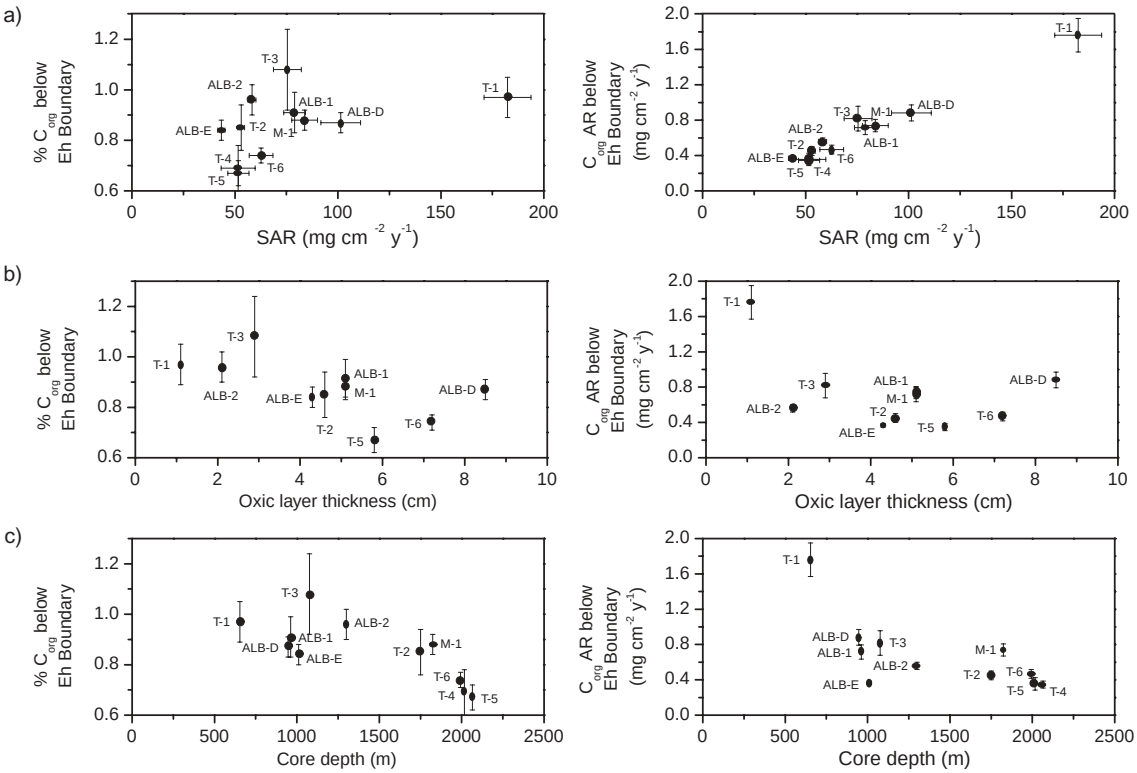

Figure 4.9. Average percentage and accumulation rate of organic carbon versus (a) mean sediment accumulation rate, (b) oxic layer thickness and (c) bottom depth of sediments from the Alboran Sea.

Degradation of organic matter once it is permanently deposited on the bottom can be assessed by comparing organic matter fluxes recorded at near bottom sediment traps and in the sediment itself below the Eh boundary. C/N values of the material collected with sediment traps at stations ALB-1 and ALB-2 (Fabres et al., 2002) increase with water depth up to 8.3 and 8.5 in the traps located only 30 meters above the seafloor, respectively (Table 4.4). These values are higher than the values recorded from the bottom sediments at these two stations, which are both below 8. Nevertheless, it has to be considered that degradation of organic matter in the water-sediment interface and above the Eh boundary implies a decrease of C/N values due to preferential consumption of carbon (respiration) respect to nitrogen (Buscail et al., 1990). This process is illustrated by the downward decreasing C/N profiles shown in Figure 4.5, which are especially clear in the Alboran Island zone sediments, and from the different degradation ratio values for C and N given in Table 4.4. From simple calculations, and assuming that no

Location	SAR (mg cm^{-2} y^{-1})	Org C AR (mg cm^{-2} y^{-1}) (%)	Org. N AR (mg cm^{-2} y^{-1}) (%)	C/N	Lithogenic AR (mg cm^{-2} y^{-1}) (%)	$CaCO_3$ AR (mg cm^{-2} y^{-1}) (%)	Org. matter AR (mg cm^{-2} y^{-1}) (%)	Opal AR (mg cm^{-2} y^{-1}) (%)
Sediment trap ALB-1-S	18.4	0.98 *(5.4%)*	0.15 *(0.8%)*	7.8	12.7 *(69%)*	2.6 *(14%)*	1.96 *(10.7%)*	1.14 *(6.2%)*
Sediment trap ALB-1-F	27.3	0.99 *(3.6%)*	0.14 *(0.5%)*	8.2	18.7 *(64%)*	5.2 *(19%)*	1.99 *(7.3%)*	1.44 *(5.3%)*
Bottom sediment ALB-1	78.9	0.72 *(0.9%)*	0.11 *(0.14%)*	7.6	63.0 *(80%)*	14.5 *(18%)*	1.43 *(1.8%)*	-
Nepheloid input (Composition)	53.6				44.3 *(83%)*	9.3 *(17%)*		
Diagenetic output (Degradation ratio)	-2.0	-0.28 *(28%)*	-0.03 *(21%)*				-0.56 *(28%)*	-1.44 *(100%)*
Balance	51.6	-0.28	-0.03		44.3	9.3	-0.56	-1.44
Sediment trap ALB-2-S	29.3	1.70 *(5.8%)*	0.28 *(1.0%)*	7.1	22.4 *(76%)*	2.4 *(8%)*	3.40 *(11.6%)*	1.08 *(3.7%)*
Sediment trap ALB-2-F	31.2	0.95 *(3.0%)*	0.13 *(0.4%)*	8.5	23.5 *(75%)*	4.7 *(15%)*	1.90 *(6.1%)*	1.06 *(3.4%)*
Bottom sediment ALB-2	58.3	0.56 *(1.0%)*	0.08 *(0.14%)*	7.9	46.9 *(80%)*	10.3 *(17%)*	1.12 *(1.9%)*	
Nepheloid input (Composition)	28.9				23.4 *(81%)*	5.5 *(19%)*		
Diagenetic output (Degradation ratio)	-1.8	-0.39 *(41%)*	-0.05 *(38%)*				-0.78 *(41%)*	-1.06 *(100%)*
Balance	27.1	-0.39	-0.05		23.4	5.5	-0.78	-1.06

Table 4.4. Comparison between accumulation rates (AR) of sediment and major constituents composition determined from sediment traps (S: 500 meters above bottom (mab); F: 30 mab) and bottom sediments (below the oxic layer) at stations ALB-1 and ALB-2. The balance accounts for what is supplied by the nepheloid layer below the bottom sediment trap plus what is degraded by early diagenesis in the oxic layer (see text). Data from sediment traps are from Fabres et al. (2002).

organic matter is supplied between the sediment trap and the bottom (see below), it can be stated that 28% and 41% of the organic matter reaching the seafloor at ALB-1 and ALB-2 stations is degraded between the water-sediment interface and the Eh boundary.

Comparing particle flux data from near bottom sediment traps from the Malaga zone with sediment accumulation rates (Table 4.4) leads as well to an insight into the important supply of material below 30 meters above the bottom on the slope and the base of the slope of the Malaga Zone. It is worth mentioning that fluxes in the sediment and in traps are obtained by two different methods covering different time scales, and differences could partly be linked to that fact. In order to quantify the amount and composition of particles that are supplied between the sediment trap and the bottom, we have assumed two premises. The first is that the amount of organic matter and opal supplied below the sediment trap is negligible. The second is that the lithogenic and carbonate materials that reach the bottom do not undergo any kind of degradation. Both premises imply that our calculations of nepheloid input below 30 m above the bottom are minimum estimates. Therefore, the amount of matter supplied below the sediment traps is calculated using the following formula:

$$Nepheloid\ input = (LAR_s - Lflux_t) + (CaCO_3AR_s - CaCO_3flux_t) \quad (5)$$

where LAR_s is the lithogenic accumulation rate in the sediment, $Lflux_t$ is the lithogenic flux to the bottom trap, $CaCO_3AR_s$ is the carbonate accumulation rate in the sediment and $CaCO_3flux_t$ is the carbonate flux to the bottom trap. The comparison reveals that as much as two thirds and half of the material accumulated at stations ALB-1 and ALB-2, respectively, is supplied between the sediment traps and the bottom. This substantial near bottom input has also been identified using the ^{210}Pb data (see previous section). Furthermore, calculated carbonate content of the particles supplied near the bottom is 17-19% (nepheloid input in Table 4.4). This composition is very similar to that of the bottom sediments recovered from this zone, and reinforces the interpretation that this material is resuspended upslope and redistributed in the basin. This inference takes us back to the premise that no organic matter is supplied below the sediment trap. If this material is resuspended elsewhere in the margin, it should have at least the same organic matter content than the margin sediments (around 1.8%). Therefore, the degradation ratio for organic matter given in Table 4.4 has to be regarded as a minimum estimate.

The third important variable regulating the abundance of organic carbon is dilution. However, dilution does not seem to be of much influence in Alboran sediments, where we find a direct relationship between percentages of organic matter and SAR (Figure 4.9a), whereas a strong dilution effect would imply an inverse one. The only exception would be core T-1, for which the SAR has been estimated to be more than twice that of most of the other studied cores (Figure 4.9a).

4.5. Conclusions

In this work, a set of eleven sediment cores collected from three different areas in the Alboran Sea (Malaga, Alboran Island and Almeria-Oran) including slope, base-of-slope and basin settings have

been investigated for a number of geochemical parameters, including Eh, ^{210}Pb, ^{137}Cs, major constituents (lithogenic, carbonates, opal and organic matter) and molecular biomarkers. The main results and conclusions that may be drawn from the above analysis are as follow.

Sediments were identified as having been accumulated mostly by hemipelagic processes. Mixing and sediment accumulation rates (SAR) in a century scale were assessed on the basis of a two-layer sedimentation model of the radiotracer profiles, and ranged from 0.2 to 15 $cm^2 \cdot y^{-1}$ and 0.043 to 0.182 $g\ cm^{-2} \cdot y^{-1}$, respectively. The water column depth and the distance from the coast appear to predominantly govern the SAR. In this sense, the high SAR in the upper slope of the Malaga area suggests the presence of a sedimentary depocenter. However, specific physiographic characteristics of each studied area do influence the sediment distribution patterns. Lithogenic constituents account for as much as 80% of the sediments accumulated in the Malaga zone, 75% in the Alboran Island zone and 70% in the Almeria-Oran zone. Carbonate concentrations show a reverse trend, being less diluted in the Almeria-Oran zone. These results reflect a combination of the influence of several different factors: the relative proximity of the studied stations to the coast and the presence of riverine inputs (in the Malaga area), active submarine canyons and physiographic barriers. The decreasing trend in mean concentrations of organic matter, mostly of marine origin, from the Malaga zone to the Almeria-Oran zone is primarily attributed to the higher production in the Western Alboran Sea. Surface production influences bottom sediment composition, as shown by the C_{37} concentrations distribution, yet near-bottom transport causes spatial homogeneity of the organic matter abundance of the sediments of a given physiographic area, disregarding small scale variability in surface waters production. Biogenic silica, on the other hand, is not efficiently preserved in bottom sediments.

Organic matter preservation appears to be controlled by oxygen availability in the water sediment interface and in the sediment itself, which is in turn controlled by the amount of oxygen of bottom waters and the SAR. A direct influence of depth, not through the SAR, but through the influence organic matter degradation during water column or near bottom transfer cannot be ruled out. Within the Malaga zone, comparisons with sediment trap data allowed to calculate minimum degradation rates of the organic matter reaching the bottom of 28% and 41% for Alb-1 (962 m depth) and Alb-2 (1300 m depth) stations, respectively. Comparison of bottom sediment and sediment trap data available from the Malaga zone also permitted us to estimate that the particle advective input below 30 meters above the bottom accounts for as much as 50-70% of the material that is ultimately deposited onto the sea floor. Higher excess ^{210}Pb fluxes than the expected export of ^{210}Pb calculated from net production on the overlaying water column, together with surface sediment concentrations and data from the sediment traps deployed in the Malaga area, denoted the significant influence of the bottom nepheloid layers on the transport and deposition of particulate matter in deep areas of the Alboran Sea.

Acknowledgements

The body of this research has been undertaken in the framework of the Mediterranean Targeted Project II - MATER (MTP II-MATER) project. We acknowledge the support of the European Commission's Marine Science and Technology (MAST) Programme under contract MAS3-CT96-0051. Substantial co-funding was obtained from the Spanish “Comisión Asesora de Investigación Científica y Técnica” and the Catalan “Comissió Interdepartamental per la Recerca i la Investigació Tecnològica”. Part of the work was finalised under the framework of the EU ADIOS project (EVK3-CT-2000-00035). The authors are very grateful to Dr. Belén Alonso and CICYT project MAYC (AMB95-0196), in the frame of which some of the sediment cores were collected. We also acknowledge the help of Belén Oliva with laboratory work. The Elemental Analysis, the ICP-AES and the Chemistry Laboratory teams of the ‘Serveis Científico Tècnics’ of Universitat de Barcelona also provided invaluable help in carbon-nitrogen and silica analyses. We want to thank the crew, technicians and scientists on board R/V García del Cid and BIO Hespérides for their assistance at sea. The 3D view of the Alboran Basin in Figure 4.1b is courtesy of J.L. Casamor. Useful comments by J.K. Cochran and S.L. Goodbred on earlier versions of the manuscript are appreciated. PM thanks the Government of Spain and the Fulbright Commission for the concession of a postdoctoral fellowship. JF was supported by a FPU grant (AP95 44002743) from the Spanish “Ministerio de Educación y Ciencia”. Both research teams are additionally funded by Generalitat de Catalunya through its excellency research groups program (ref. 1999 SGR-63).

References

Alonso, B. and Maldonado, A., 1992. Plio-Quaternary margin growth patterns in a complex tectonic setting: northeastern Alboran Sea. Geo-Marine Letters, 12 (2-3), 137-143.

Arnone, R.A., La Violette, P.E., 1986. Satellite definition of the bio-optical and thermal variation of the coastal eddies associated with the African current. Journal of Geophysical Research, 91, 2351-2364.

Arnone, R.A., Wiesenburg, D.A., Saunders, K.D., 1990. The origin and characteristics of the Algerian Current. Journal of Geophysical Research, 95 (C2), 1587-1598.

Baldacci, A., Corsini, G., Grasso, R., Manzanella, G., Allen, J. T., Cipollini, P., Guymer, T. H., Snaith, H. M., 2001. A study of the Alboran sea mesoscale system by means of empirical orthogonal function decomposition of satellite data. Journal of Marine Systems, 29, 293-311.

Bárcena, M. A., Abrantes, F., 1998. Evidence of a high-productivity area off the coast of Malaga from studies of diatoms in surface sediments. Marine Micropaleontology, 35, 91-103.

Bárcena, M. A, Cacho, I, Abrantes, F., Sierro, F. J, Grimalt, J. O., Flores, J. A., 2001. Paleoproductivity variations related to climatic conditions in the Alboran Sea (western Mediterranean) during the last glacial–interglacial transition: the diatom record. Palaeogeography, Palaeoclimatology, Palaeoecology, 167 (3-4), 337-357.

Benninger, L.K., Aller, R.C., Cochran, J.K., Turekian, K.K., 1979. Effects of biological mixing on the ^{210}Pb chronology and trace metal distribution in a Long Island Sound sediment core. Earth and Planetary Science Letters, 43, 241-259.

Berman, S., 1990. Marine sediment reference materials for trace metals and other constituents. Marine Analytical Chemistry Standards Program, Division of Chemistry, National Research Council, Otawa, Ontario, K1AOR6, 4 pp.

Buscail, R., Pocklington, R., Daumas, R., Guidi, L., 1990. Fluxes and budget of organic matter in the benthic boundary layer over the Northwestern Mediterranean margin. Continental Shelf Research, 10 (9-11), 1089-1122.

Buscail, R., Ambatsian, P., Monaco, A., Bernat, M., 1997. ^{210}Pb, manganese and carbon: indicators of focussing processes on the nortwestern Mediterranean continental margin. Marine Geology, 137, 271-286.

Cacho, I., Grimalt, J, O., Pelejero, C., Canals, M., Sierro, F. J., Flores, J. A., Shackleton, N., 1999. Dansgaard-Oeschger and Heinrich Event imprints in Alboran Sea paleotemperatures. Paleoceanography, 14 (6), 698-705.

Carter, T.G, Flanagan, J.P., Jones, C.R., Marchant, F.L., Murchinson, R.R., Rebman, J.H., Sylvester, J.C., Whitney, J.C., 1972. A new bathymetric chart and physiography of the Mediterranean Sea. In: Stanley, D.J. (Ed.), The Mediterranean Sea: A Natural Sedimentation Laboratory. Dowden, Hutchison and Ross, Inc., Stroudsburg, PA, pp. 1-24.

Chester, R., 1990. Marine Geochemistry. Unwin Hyman Ltp. publ., London.

Cochran, J.K., 1985. Particle mixing rates in sediments of the eastern equatorial Pacific. Evidence from ^{210}Pb, ^{239,240}Pu and ^{137}Cs distributions at MANOP sites. Geochimica et Cosmochimica Acta, 45, 1155-1172.

DeMaster, D.J., Cochran, J.K., 1982. Particle mixing rates in deep-sea sediments determined from excess ^{210}Pb and ^{32}Si profiles. Earth and Planetary Science Letters, 61, 257-271.

Durrieu de Madron, X., Nyffeler, F., Godet, C.H., 1990. Hydrographic structure and nepheloid spatial distribution in the Gulf of Lions continental margin. Continental Shelf Research, 10, 915-929.

Eglinton, G., Hamilton, R. J., 1967. Leaf epicuticular waxes. Science, 156, 1322-1335.

Ercilla, G., Alonso, G., Baraza, J.. 1994. Post-Calabrian sequence stratigraphy of the northwestern Alboran Sea (southwestern Mediterranean). Marine Geology, 120, 249-265.

Fabres, J., Calafat, A., Sànchez-Vidal, A., Canals, M., Heussner, S., 2002. Composition and spatio-temporal variability of particle fluxes in the Western Alboran Gyre, Mediterranean Sea. Journal of Marine Systems, 33-34, 431-456.

Falkowski, P. G., Behrenfeld, M. J., Kolber, D. K., 2002. Ocean Primary Productivity Study. Estimated Annual Global Primary Production Maps. http://marine.rutgers.edu/opp/

Font, J., 1987. The path of the Levantine Intermediate Water to the Alboran Sea. Deep-Sea Research, 34, 1745-1756.

Froelich P. N., Klinkhammer, G. P., Bender, M. L., Luedtke, N. A., Heath, G. R., Cullen, D., Dauphin, P., Hammond, D., Hartman, B., Maynard, V., 1979. Early oxidation of organic matter in pelagic

sediments of the eastern equatorial Atlantic: suboxic diagenesis. Geochimica et Cosmochimica Acta, 43, 1075-1090.

Garcia-Gorriz, E., Carr, M.-E., 1999. The climatological annual cycle of satellite-derived phytoplankton pigments in the Alboran Sea. Geophysical Research Letters, 26 (19), 2985-2988.

Gascard, J.C. and Richez, C. 1985. Water mass and circulation in the Western Alboran Sea and in the Strait of Gibraltar. Progress in Oceanography, 15, 157-216.

Goldberg, E.D., Koide, M., 1962. Geochronological studies of deep-sea sediments by the ionium-thorium method. Geochimica et Cosmochimica Acta, 26, 417-450.

Guinasso, N.L., Shink, D.R., 1975. Quantitative estimates of biological mixing rates in abyssal sediments. Journal of Geophysical Research, 80 (21), 3032-3043.

Huang, T.-C., Stanley, D. J., 1972. Western Alboran Sea: Sediment dispersal, ponding and reversal of currents. Stanley, D.J. (Ed.), The Mediterranean Sea: A Natural Sedimentation Laboratory. Dowden, Hutchison and Ross, Inc., Stroudsburg, PA, pp. 521-559.

Kinder, T.H., Parrilla, G., 1987. Yes, Some of the Mediterranean Outflow Does Come From Great Depth. Journal of Geophysical Research, 92(C3), 2901-2906.

La Violette, P.E., 1986. Short-term measurements of surface currents associated with the Alboran Sea gyre during Donde Va?. Journal of Physical Oceanography, 16 (2), 262-279.

La Violette, P.E., 1990. The Western Mediterranean Circulation Experiment (WMCE): Introduction. Journal of Geophysical Research, 95 (C2), 1511-1514.

Leclaire, L., 1972. Aspects of Late Quaternary sedimentation on the Algerian Precontinent and in the adjacent Algiers-Balearic Basin. In: Stanley, D.J. (Ed.), The Mediterranean Sea: A Natural Sedimentation Laboratory. Dowden, Hutchison and Ross, Inc., Stroudsburg, PA, pp. 561-582.

Liu, K.K., Atkinson, L., Chen, C.T.A., Gao, S., Hall, J., Macdonald, R.W., Talaue McManus, L., Quiñones, R., 2000. Exploring continental margin carbon fluxes on global scale. EOS, 81 (52), 641-644.

Lorenz, S.E., Wiesenburg, D.A, De Palma, I., Kenneth, S.J., Gustafson, D.E., 1998. Interrelationships among primary production, chlorophyll and environmental conditions in frontal regions of the western Mediterranean Sea. Deep-Sea Research. 35 (5), 793-810.

Masqué, P., Isla, E., Sanchez-Cabeza, J.A., Palanques, A., Bruach, J.M., Puig, P., Guillén, J., 2002. Sediment accumulation rates and carbon fluxes to bottom sediments at the western Bransfield Strait (Antarctica). Deep-Sea Research II, 49 (4-5), 921-933.

Molero, J., Sanchez-Cabeza, J.A., Merino, J., Mitchell, P.I., Vidal-Quadras, A., 1999. Impact of ^{134}Cs and ^{137}Cs from the Chernobyl reactor accident on the Spanish Mediterranean marine environment. Journal of Environmental Radioactivity, 43, 357-370.

Moran, X. A. G., Estrada, M., 2001. Short-term variability of photosynthetic parameters and particulate and dissolved primary production in the Alboran sea (SW Mediterranean). Marine Ecology Progress Series, 212, 53-67.

Morel, A., André, J. M. 1991. Pigment distribution and primary production in the western Mediterranean as derived and modeled from Coastal Zone Color Scanner observations. Journa of Geophysical Research, 96, 12685-12698.

Nieuwenhuize, J., Maas, Y.E.M., Middelburg, J.J., 1994. Rapid analysis of organic carbon and nitrogen in particulate materials. Marine Chemistry, 45, 217-224.

Nittrouer, C.A., DeMaster, D.J., McKee, B.A., Custhall, N.H., Larsen, L.I., 1984. The effect of sediment mixing on ^{210}Pb accumulation rates for the Washington continental shelf. Marine Geology, 31, 297-316.

Palanques, A., Sanchez-Cabeza, J.A., Masqué, P., León, L., 1998. Historical record of heavy metals in a highly contaminated Mediterranean deposit: The Besòs prodelta. Marine Chemistry, 61, 209-217.

Papucci, C., Charmasson, S., Delfanti, R., Gascó, C., Mitchell, P., Sánchez-Cabeza, J.A., 1996. Time evolution and levels of man-made radioactivity in the Mediterranean Sea. In: Guéguéniat, P., Germain, P., Métivier, H. (Eds.), Radionuclides in the Oceans. Les Éditions de Physique, Les Ulis, France, 1996, pp. 177-197.

Parrilla, G., Kinder, T.H., Preller, R.H., 1986. Deep and Intermediate Mediterranean Water in the western Alboran Sea. Deep Sea Research, 33, 55-88.

Parrilla, G., Kinder, T.H. 1987. The physical oceanography of the Alboran Sea. NORDA report, 184, 26 pp.

Pistek, P., De Strobel, F., Montanari, C., 1985. Deep-sea circulation in the Alboran Sea. Journal of Geophysical Research, 90 (C3), 4969-4976.

Radakovitch O., Heussner S., 1999. Fluxes and budget of ^{210}Pb on the continental margin of the Bay of Biscay (Northeastern Atlantic). Deep-Sea Research II, 46 (10-11), 2175-2203.

Rey, J., Medialdea, T., 1989. Los sedimentos cuaternarios superficiales del margen continental español. Publicaciones Especiales del Instituto Español de Oceanografía, 3, 36 pp.

Roberts, K.A., Cochran, J.K., Barnes, C., 1997. ^{210}Pb and ^{239,240}Pu in the Northeast Water Polynya, Greenland: particle dynamics and sediment mixing rates. Journal of Marine Systems, 10, 401-413.

Ruiz, J., Echevarria, F., Font, J., Ruiz, S., García, E., Blanco, J.M., Jiménez-Gómez, F., Prieto, L., González-Alaminos, A., García, C. M., Cipollini, P., Snaith, H., Bartual, A., Reul, A., Rodríguez, V., 2001. Surface distribution of chlorophyll, particles and gelbstoff in the Atlantic jet of the Alboran Sea: from submesoscale to subinertial scales of variability. Journal of Marine Systems, 29, 277-292.

Sanchez-Cabeza, J.A., Masqué, P., Ani-Ragolta, I., 1998. ^{210}Pb and ^{210}Po analysis in sediments and soils by microwave acid digestion, Journal of Radioanalytical and Nuclear Chemistry, 227, 19-22.

Sanchez-Cabeza, J.A., Masqué, P., Ani-Ragolta, I., Merino, J., Frignani, M., Alvisi, F., Palanques, A., Puig, P. 1999a. Sediment accumulation rates in the southern Barcelona continental margin (NW Mediterranean Sea) derived from ^{210}Pb and ^{137}Cs chronology. Progress in Oceanography 441 (1-3), 313-332.

Sanchez-Cabeza, J.A., Masqué, P., Mir, J., Martínez-Alonso, M., Esteve, I., 1999b. ^{210}Pb atmospheric flux and mat growth rates of a microbial mat from the northwestern Mediterranean Sea area (Ebro river delta). Environmental Science and Technology, 33, 3711-3715.

Sarhan, T., García-Lafuente, J., Vargas, M., Vargas, J.M.. Plaza, F. 2000. Upwelling mechanisms in the Northwestern Alboran Sea. Journal of Marine Systems, 23, 317-331.

Shepard, F. P., 1954. Nomenclature based on sand-silt-clay ratios. Journal of Sedimentary Petrolology, 24, 151-158.

Smith, J.M., 2001. Why should we believe ^{210}Pb sediment geochronologies?. Journal of Environmental Radioactivity, 55, 121-123.

Stanley, D. J., Gehin, C. E., Bartolini, C. 1970. Flysch-type sedimentation in the Alboran Sea, Western Mediterranean. Nature, 228, 979-983.

Stanley, D. J., Kelling, G., Vera, J. A., Sheng, H. 1975. A model of input in a deep marine basin. Smithsonian Contributions to the Earth Sciences, 15, 51 pp.

Tintoré, J., La Violette, P.E., Bladé, I., Cruzado, A., 1988. A study of an intense density front in the eastern Alboran Sea: The Almeria-Oran front. Journal of Physical Oceanography, 18, 1384-1397.

Tintoré, J., Viúdez, A., Gomis, D., Alonso, S., Werner, F.E., 1994. Mesoscale variability and Q vector vertical motion in the Alboran Sea. In: Seasonal and Interannual Variability of the Western Mediterranean Sea. Coastal and Estuarine Studies, 46, 47-71.

Tysson, R.V., 2001. Sedimentation rate, dilution, preservation and total organic carbon: some results of a modelling study. Organic Geochemistry, 32, 333-339.

UNSCEAR, 2000. Sources and effects of ionizing radiation, Ionizing Radiation: Sources and Biological Effects, United Nations, New York.

Villanueva, J., Grimalt, J. O., 1997. Gas chromatographic tuning of the UK'37 paleothermometer. Analytical Chemistry, 69, 3329-3332.

Viúdez, A., Tintoré, J., 1995. Time and space variability in the eastern Alboran Sea from March to May 1990. Journal of Geophysical Research, 100, 8571-8586.

Viúdez, A., Tintoré, J., Haney, R.L., 1995. Circulation in the Alboran Sea as determined by quasi-synoptic hydrographic observations. Part I: Three dimensional structure of the two anticyclonic gyres. Journal of Physical Oceanography, 26, 684-705.

Volkman, J. K., Eglinton, G., Corner, E. D. S., Sargent, J. R., 1980. Novel unsaturated straight-chain C37-C39 methyl ethyl ketones in marine sediments and coccolithophore Emiliania huxleyi. In: Douglas, A. G., Maxwell, J. R. (Eds.), Advances in Organic Geochemistry, Pergamon Press, Oxford , UK, pp. 219-228.

Zamarreño, I., Vázquez, A., Maldonado, A. 1983. Sedimentación en la plataforma de Almería: Un ejemplo de sedimentación mixta silícico-carbonatada en clima templado. In: Estudio oceanográfico de la plataforma continental española. E.O.P.C. Seminario interdisciplinar (Cádiz 15-18 Marzo). pp. 97-120.

Zuo, Z., Eisma, D., Gieles, R., Beks, J. 1997. Accumulation rates and sediment deposition in the northwestern Mediterranean. Deep-Sea Research II, 44, 597-609.